journal of the international meteor organization

WGN

42:3
june 2014

New showers found in CMN and SonotaCo databases
First results of the 2014 Camelopardalids
Persistent fireball over the British Isles
February–March video meteors

ISSN 1016-3115

WGN Vol. 42, No. 3, June 2014, pp. 87 – 126

Administrative

Meteor Science

Preliminary results

Front cover photo

This Camelopardalid in the constellation of Draco was filmed at 25 frames/s from the center of München, Germany at $01^{h}58^{m}08^{s}$–13^{s} UT on 2014 May 24, using a Canon EOS C300 Digital Cinema Camera with Zeiss High Speed Cine Distagon 1.2/18 mm lens, set at ISO 20 000. This compilation shows each video frame displaced by 5 pixels, projected in such a way that the meteor moves from left to right and top to bottom. Persistent emission and wake is visible, as is the sudden deceleration when the meteoroid breaks. Original recording by Peter C. Slansky; compilation by Jim Albers and Peter Jenniskens.

Writing for WGN

This Journal welcomes papers submitted for publication. All papers are reviewed for scientific content, and edited for English and style. Instructions for authors can be found in WGN **31:4**, 124–128, and at `http://www.imo.net/docs/writingforwgn.pdf` .

Copyright

Legal address

International Meteor Organization, Jozef Mattheessensstraat 60, 2540 Hove, Belgium.

News from the IMO Commissions

Cis Verbeeck[1]

In name of the IMO Council, it is my pleasure to announce some recent and upcoming changes in IMO's Commissions.

From the publication of the present June issue of 2014 onwards, Bill Ward is the new Director of the Photographic Commission. While this Commission was in dormant mode for many years as video observations gained terrain on photographic observations, there is an important place for still image meteor photography with a DSLR. In the present issue of WGN, Bill describes at length how you can contribute to the various goals of the Photographic Commission. Welcome aboard Bill! We wish you and the Photographic Commission a lot of success.

Since no single telescopic meteor observation was reported to IMO in the past ten years, the Commission Director Malcolm Currie acknowledged that this way of observing meteors has become obsolete. Together with him, the Council decided to abolish the Telescopic Commission.

IMO's Fireball DAta Center FIDAC has also been virtually out of business for the past years and is abolished as well. Behind the scenes however, Mike Hankey and Vincent Perlerin have been working hard to set up an online multi-language fireball form (with the help of many other IMO members). This development is nearly finished, and we will be proud to announce it at the IMC in Giron.

The Council would like to thank Malcolm Currie, Marc de Lignie, and André Knöfel for all the work they invested in the Telescopic Commission, the Photographic Commission, and the Fireball DAta Center, respectively.

For the Visual, Video, and Radio Commissions, no changes are in place.

Practical, updated information on the Commissions can be found — as always — in the inside back cover of WGN and on the IMO website.

Meanwhile, enjoy this issue of WGN!

IMO bibcode WGN-423-verbeeck-commissions NASA-ADS bibcode 2014JIMO...42...87V

Photographic Commission: Future Plans

Bill Ward [2]

As I take over the position of Director of the Photographic Commission I hope that with the help of IMO members the Commission can once again be a source of both nice pictures and useful images. The Commission must exist to help and encourage all levels of meteor observer to get the best from their efforts.

Recently meteor observing has been dominated by video work. It is easy to understand why. Relatively low cost, ease of operation (almost fully automatic) and data reduction performed by established software packages. Most major aspects of meteor astronomy can be addressed by video work so consequently "meteor photography" has been in decline as a source of observations and data.

However "meteor photography" has been undergoing its own albeit smaller revolution thanks to the consumer Digital SLR (DSLR). The modern DSLR is a much more efficient and importantly linear detector of photons. Gone are the difficulties of emulsion film processing and the efforts of trying to measure images on negatives or prints. That the image is in a digital format means it is immediately available for image processing, measurement and reduction.

Perhaps the key issue is that the DSLR is now commonplace. This large number offers much potential if observers can be mobilised to work in a coordinated way. The Photographic Commission must now focus on exploiting digital techniques rather than film.

Given the utility of video cameras how can DSLR imaging fit into a programme of observing within the IMO?

1. Many casual observers take meteor images for the challenge of catching an elusive target alone. The Commission should set about building a library of "pretty pictures". This would give the casual observer who records an meteor image somewhere to send it. It can be archived and it will also provide material for WGN, IMO promotional material and perhaps some conference uses.

[1] Bogaertsheide 5, 2560 Kessel, Belgium. Email: cis.verbeeck@scarlet.be

[2] School of Engineering, University of Glasgow, Glasgow, G12 8LT, UK. Email: william.ward@glasgow.ac.uk

2. Purely aesthetic images can go from pretty picture to something of a little more value if a standard reporting system is adopted. Again the utility of the DSLR istelf comes into play. Every image is date and time stamped so we have immediate temporal information. If regular imaging can be encouraged together with the additional data, we have another avenue with which to examine fireballs. Again, it is the route of having a known path of submission. A random image might be of limited value but tied to other reports it becomes much more significant.

3. Much of the older IMO material regarding meteor spectroscopy is from emulsion based experience combined with glass prisms. Glass prisms have the advantage of only producing one spectrum image. Unfortunately this spectrum is of non uniform dispersion. Combined with the difficulties of capturing a spectrum in the first place the techniques of measuring the spectrum and interpolating the wavelength measurements made meteor spectroscopy rather esoteric.

   Today cheap plastic grating material is readily available and easy to mount in front of a lens. Due to the nature of light passing through the grating material multiple spectra are produced. In any given field of view it is usually the first order that will be captured since it is the brightest. DSLR meteor images also tend to be of better quality than those obtained by video methods. Typically the image and wavelength resolution is superior. The digital images are pre-processed with an image processing package then exported to a spectral analysis program. All of this software can be found free of charge! To be useful for taxonomy it is not merely the spectrum as a whole that is interesting but the photometrically reduced images allow line ratios to be determined. This is a demanding challenge but the nature of DSLR images makes it possible.

4. Still imaging is the best way to examine meteor trains. Some old assumptions about meteor trains can now be re-examined as digital photography offers an unprecedented technique to image and study meteor trains. It has been long held that meteor trains were only generated by fast meteors. There is now evidence that they are much more common. Video systems are generally incapable of capturing such events.

Under the broad title of Photographic Commission the use of CCDs should now be included as standard. Smaller chipped cameras equipped with CCTV type objectives can produce excellent results. This is especially true in the spectroscopy where the higher bit resolution gives greater detail in the line and line ratio measurements. Larger CCD cameras equipped with 35 mm format lenses can be powerful instruments.

Examples of all this have appeared in WGN or at the IMC over recent years. Mostly they have been in isolation. It must be the goal of the Photographic Commission to encourage all meteor observers who have a DSLR camera to make use of its potential and tie together the results. The first objective of the Commission will be to provide a route for meteor imagers to submit images to a properly coordinated IMO Meteor Image Archive. This will provide the IMO with a whole new set of data to use.

IMO bibcode WGN-423-ward-photographic NASA-ADS bibcode 2014JIMO...42...87W

Visual meteor observation data handling

Jürgen Rendtel[1] *and Geert Barentsen*[2]

One of the most interesting results obtained from systematic global visual meteor observations is the possibility to derive detailed profiles of the population index r, the ZHR and the spatial number density or meteoroid flux, respectively, across the Earth's path through the streams. This requires that the data is as complete as possible within a reasonable time after the observations. Over the last years, the IMO's webpage offered an on-line report form so that observers could send their data immediately after the observation. Further, this allowed an instantaneous analysis, resulting in live ZHR graphs[a], so that everyone could immediately follow the activity profile of showers. This, of course, can serve as a motivation to carry out regular observations.

The shown profiles have been marked as preliminary results for several reasons. The major reason is that the ZHR was calculated assuming a constant, 'tabulated' or an average population index r for the entire period rather than the profile found for the shower under study. It is well known that in most cases we find a difference of the particle size distribution between the centre of a meteoroid stream and its outer regions. In the best case

[1] Eschenweg 16, D-14476 Marquardt, Germany. Email: jrendtel@aip.de
[2] University of Hertfordshire, Hatfield AL10 9AB, UK. Email: geert@barentsen.be
[a] http://www.imo.net/zhr

the live analysis could be done with an assumed average profile. During many studies we have learned that this profile is subject to variations and we need to calculate a reliable r-profile first.

Another reason for the preliminary nature of the live ZHR graphs is that, before any reliable analysis can be done, it is important to check the data for entry errors. For example, an observer may accidentally mix longitude and latitude or omit a minus sign. When looking at the geographical distribution of the observing locations shown on the webpage one immediately sees obvious errors, but others may remain undetected. So the quality check is an important part.

For comprehensive analyses and quality control to be carried out, it is necessary that the observation reports are archived in a database. For this purpose, the Visual Meteor DataBase (VMDB[b]) was created many years ago. The VMDB is a database application created using the dBase platform. It is accompanied by a series of user interfaces and data analysis scripts. Unfortunately, the application was created long before the internet became popular, and at present it is not possible to enter, correct or query the data online. This situation is not ideal: too much manual labour is required to keep the database up to date, and to make the collected data accessible to the world.

Hence, we are looking for volunteers to help improve the situation. On one hand, we need software engineers to create a modern, web-based database application to curate the visual meteor observing reports. On the other hand, we also welcome volunteers to help out with the quality checking of the data. Once this is done and we have the checked data available, we will provide it on the IMO webpage. This will allow to continue the series of detailed shower analyses and to look for undetected features within the streams. Any interested people should contact the authors.

IMO bibcode WGN-423-rendtel-visual NASA-ADS bibcode 2014JIMO...42...88R

Call for observations of κ-Cygnids in 2014

WGN Editorial board

In an upcoming paper, Masahiro Koseki calls for observations of the κ-Cygnids.

Some previous observations of the shower point at a possible periodic nature of the shower.

Assuming the 7-year period, this year may see enhanced activity from the κ-Cygnids. Based on past returns presented in the submitted paper, activity may be enhanced between $\lambda_\odot$ 133° and 147°.

The radiant (KCG1 and KCG2 drifts in Figure 1) should lie close to the location published in the IMO Meteor Shower Calendar.

Observers are encouraged to keep an eye on the possible enhancement, employing visual and instrumental techniques.

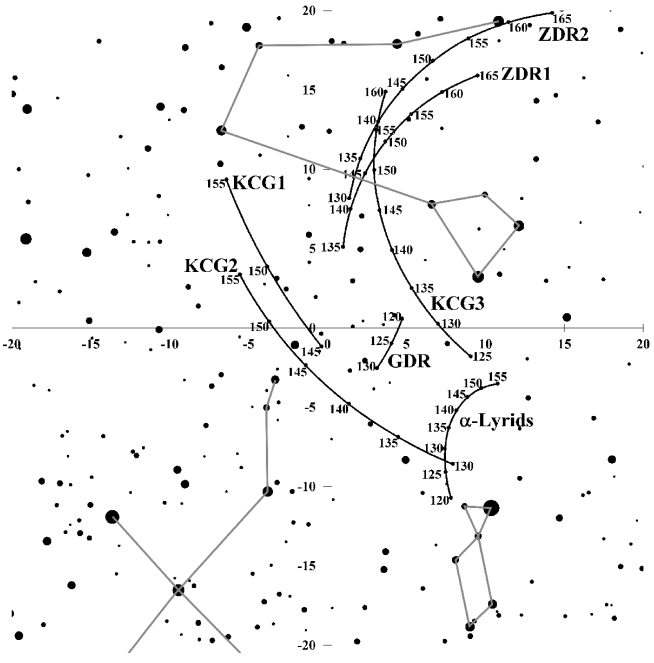

Figure 1 – Radiant drifts of the Cygnids-Draconids Complex plotted on a star chart.

IMO bibcode WGN-423-wgn-kcgcall NASA-ADS bibcode 2014JIMO...42...89W

[b] http://www.imo.net/data/visual

Meteor Science

Results of CMN 2013 search for new showers across CMN and SonotaCo databases I

Željko Andreić[1], *Peter Gural*[2], *Damir Šegon*[3], *Ivica Skokić*[4], *Korado Korlević*[5], *Denis Vida*[6], *Filip Novoselnik*[7], *and David Gostinski*[8]

The first results of a search that compared each meteor to all others in the same database are presented. The database was constructed by combining Croatian Meteor Network databases for 2007 to 2010 and SonotaCo databases for 2007 to 2011. The most significant 24 possible new showers are described in this article.

Received 2013 November 27

1 Introduction

The search described in this paper was initiated by the assumption that one meteor is 'the parent body' and minor stream correlations were then made by finding statistically significant associations of this particular 'parent body' to meteors from our combined database. As a result, each meteor orbit was compared to all other orbits, using several D-criterion methods as the measure of the similarity of the two orbits, namely D_{SH} (Southworth & Hawkins, 1963), D_D (Drummond, 1981) and D_H (Jopek, 1993). The orbits were claimed to be similar if $D_{SH} < 0.15$, $D_H < 0.15$ and $D_D < 0.075$. All three criteria have to be satisfied simultaneously.

The database that was used in the search described here is the same database as in Šegon et al. (2014a), containing over one hundred thousand meteoroid orbits (114 280 from SonotaCo 2007–2011 catalogues plus 19 372 from CMN 2007–2010 catalogues). However, while in the search described by Šegon et al. (2014a) a minor body (comet or Near-Earth Object) orbit was used as a starting point to search for members of a possible minor meteor shower, in the work described here a single meteor orbit from the same database was used as a starting point, requiring a more elaborate search pattern described below. The detailed description of the search method is also given in our paper presented at the Meteoroids 2013 conference (Šegon et al., 2014b).

Additionally, the IMO video meteor database (International Meteor Organization, 2012) that contains nearly one and a half million single station records (1993–2012) was used to provide further statistical relevance to a given shower's existence. Both datasets cover radiants down to declination −30°.

An initial run produced a very long list of possible meteor groups (at this stage we do not call them potential showers yet). We set the low limit of the number of meteors in one group to 10. Altogether 56 486 meteors (out of 133 652) were grouped in one of 3172 groups.

In the following runs the groups were sorted by the number of meteors in the group, and the mean orbit for each group was calculated. After that, groups with similar mean orbits were eliminated, leaving only the largest one in the procedure. Finally, starting from the largest group, meteors that belong to it were eliminated from the search, the remaining meteors were checked for association with the next available group, etc.

At the end, the groups were studied individually and a list of potential new minor showers was formed. The potential showers were sorted according to the number of orbits per degree of solar longitude, those with the most orbits being put onto the top of the list. In this way, a final list of 72 potential showers was obtained. The first 24 are described in this paper and the next 48 will be described in two follow-up papers.

Lastly, it should be noted that these results should be reevaluated by working with a different and larger database of meteor orbits that have been accumulated in recent years. Also comparison should be made against the results of other groups doing similar research (e.g. CAMS, EDMOND and similar). The reason is that the use of multiple D-criteria with strict tolerances to determine the similarity of orbits does not always guarantee that the orbits are really part of a stream and not simply chance alignments. So further investigation and analysis are needed on each candidate stream to either confirm or reject the associated meteors belonging to a genuine new shower.

[1]University of Zagreb, Faculty of Mining, Geology and Petroleum Engineering, Pierottijeva 6, 10000 Zagreb, Croatia. Email: zandreic@rgn.hr

[2]351 Samantha Drive, Sterling, VA 20164-5539, USA. Email: peter.s.gural@leidos.com

[3]Astronomical Society Istra Pula, Park Monte Zaro 2, 52100 Pula, Croatia.
Višnjan Science and Education Center, Istarska 5, 51463 Višnjan, Croatia. Email: damir.segon@pu.htnet.hr

[4]Astronomical Society "Anonymus", B. Radića 34, 31550 Valpovo, Croatia and Faculty of Electrical Engineering, University of Osijek, Kneza Trpimira 2B, 31000 Osijek, Croatia. Email: ivica.skokic@gmail.com

[5]Višnjan Science and Education Center, Istarska 5, 51463 Višnjan, Croatia. Email: korado@astro.hr

[6]Astronomical Society "Anonymus", B. Radića 34, 31550 Valpovo, Croatia and Faculty of Electrical Engineering, University of Osijek, Kneza Trpimira 2B, 31000 Osijek, Croatia. Email: denis.vida@gmail.com

[7]Astronomical Society "Anonymus", B. Radića 34, 31550 Valpovo, Croatia and Faculty of Electrical Engineering, University of Osijek, Kneza Trpimira 2B, 31000 Osijek, Croatia. Email: novoselnikf@gmail.com

[8]Astronomical Society "Anonymus", B. Radića 34, 31550 Valpovo, Croatia and Faculty of Electrical Engineering, University of Osijek, Kneza Trpimira 2B, 31000 Osijek, Croatia. Email: david.gostinski1@gmail.com

IMO bibcode WGN-423-andreic-showers1
NASA-ADS bibcode 2014JIMO...42...90A

Table 1 – Mean orbits of the new showers. ID and name are the IAU identification and name of the shower, $\lambda_\odot$ solar longitudes of the activity period, $\overline{\lambda_\odot}$ average solar longitude, RA and DEC are coordinates of the mean radiant, dRA and dDEC are daily motion of the radiant in RA and DEC, v_g is geocentric velocity, q perihelion distance, e eccentricity, ω argument of perihelion, Ω longitude of ascending node, i inclination and N is the number of identified orbits. The error values are standard deviations of the corresponding value. In the case of RA and DEC there is a contribution of the daily motion to the dispersion of the radiants. All angular values are given in degrees, and v_g is in km/s.

ID	name	$\lambda_\odot$	$\overline{\lambda_\odot}$	RA	DEC	dRA	dDEC	v_g	q	e	ω	Ω	i	N
548 FAQ	15 Aquariids	103–120	113	318.2 ± 3	-2.1 ± 1.6	0.84	0.23	37.7±1.3	0.140±0.011	0.929±0.017	322.2±2	112.7±3	34.8±2.8	39
549 FAN	49 Andromedids	108–122	114	20.9 ± 4	46.7 ± 2.0	0.90	0.32	60.1±1.1	0.918±0.016	0.925±0.056	143.1±3	114.0±4	118.2±2.8	35
550 KPC	κ Cassiopeiids	114–122	119	10.5 ± 3	64.2 ± 2.9	0.64	0.40	50.2±1.9	0.970±0.011	0.908±0.035	155.0±3	119.0±3	90.0±4.3	16
551 FSA	47 Andromedids	131–146	139	22.4 ± 4	38.6 ± 2.2	0.95	0.20	63.7±1.1	0.910±0.019	0.929±0.059	217.9±4	138.6±4	132.0±4.0	36
553 DPE	δ Perseids	159–177	168	58.5 ± 4	46.7 ± 1.9	0.89	0.18	64.5±0.8	0.910±0.026	0.922±0.052	216.6±5	168.4±5	134.0±3.2	35
554 APE	α Perseids	166–178	171	50.3 ± 4	49.3 ± 2.2	0.96	0.33	61.4±1.2	0.796±0.026	0.941±0.049	235.2±3	171.2±4	123.9±3.8	31
555 OCP	October γ Camelopardalids	189–196	191	63.3 ± 9	72.9 ± 1.8	2.62	0.15	50.8±1.5	0.897±0.019	0.948±0.053	217.8±4	191.3±2	89.7±3.8	16
556 PTA	ϕ Taurids	187–198	193	63.9 ± 4	29.1 ± 1.1	1.15	0.20	60.2±0.9	0.234±0.019	0.973±0.031	303.7±2	193.1±3	156.3±2.9	22
557 SFD	64 Draconids	208–223	216	302.9 ± 5	65.6 ± 2.5	−0.50	−0.10	26.4±1.2	0.972±0.008	0.961±0.057	196.6±4	216.4±5	38.4±2.3	37
558 TSM	27 Monocerotids	215–229	221	117.9 ± 3	-6.1 ± 1.4	0.79	−0.04	64.2±0.9	0.918±0.020	0.842±0.045	32.9±5	41.3±4	132.8±2.9	29
559 MCB	β Canis Majorids	233–242	237	94.4 ± 3	-21.5 ± 1.7	0.78	0.14	44.2±1.5	0.618±0.029	0.930±0.049	77.2±4	56.8±3	71.5±3.3	20
560 SES	17 Sextantids	251–271	262	150.8 ± 4	-6.9 ± 2.1	0.71	−0.22	67.1±0.7	0.782±0.039	0.929±0.051	54.9±6	82.0±6	146.8±3.6	39
561 SSX	6 Sextantids	251–273	262	146.5 ± 5	-1.9 ± 1.6	0.82	−0.18	66.4±0.9	0.617±0.037	0.966±0.046	76.1±5	82.4±6	150.2±3.1	44
562 BCT	13 Comae Berenicids	255–275	265	186.1 ± 3	26.2 ± 2.6	0.69	−0.39	65.9±1.1	0.982±0.003	0.871±0.059	183.8±4	265.4±5	134.6±3.7	50
563 DOU	December ω Ursae Majorids	263–275	269	159.5 ± 4	43.0 ± 1.8	1.11	−0.40	56.7±1.2	0.534±0.027	0.970±0.049	265.9±3	269.0±3	106.9±2.8	50
564 SUM	61 Ursae Majorids	270–284	275	180.4 ± 3	35.6 ± 2.5	0.85	−0.35	61.0±1.3	0.785±0.018	0.934±0.053	234.4±3	275.2±4	118.7±3.9	33
565 FUM	59 Ursae Majorids	271–285	278	174.2 ± 4	43.9 ± 2.5	0.88	−0.43	55.1±1.3	0.648±0.023	0.955±0.045	252.5±3	277.8±4	100.7±3.4	36
566 BCF	5 Comae Berenicids	271–288	278	184.0 ± 3	20.4 ± 2.2	0.66	−0.27	67.4±0.9	0.863±0.029	0.932±0.055	221.5±5	278.1±4	143.4±3.4	36
567 XHY	ξ Hydrids	278–289	284	171.6 ± 4	-28.0 ± 1.9	1.02	−0.21	64.6±1.1	0.931±0.012	0.903±0.047	27.3±3	104.0±3	129.4±3.6	26
568 FCV	14 Canum Venaticids	306–313	309	200.9 ± 3	29.4 ± 1.5	0.94	−0.53	56.2±1.1	0.627±0.029	0.941±0.050	255.5±3	308.9±2	104.7±2.1	17
569 OHY	o Hydrids	302–316	309	176.3 ± 3	-34.1 ± 1.9	0.80	−0.38	59.1±1.0	0.684±0.025	0.931±0.039	68.6±3	128.9±4	114.3±3.0	29
570 FBH	February β Herculids	309–318	313	247.9 ± 2	24.6 ± 1.7	0.81	−0.10	54.9±1.3	0.904±0.013	0.930±0.061	146.0±3	313.1±2	99.1±3.3	24
571 TSB	26 Bootids	341–345	344	217.6 ± 2	24.0 ± 1.0	0.60	−0.05	49.7±0.8	0.498±0.023	0.968±0.044	270.7±2	343.5±1	83.9±1.8	10
572 TOH	21 Herculids	348–353	350	246.2 ± 1	7.6 ± 1.4	0.27	0.14	63.7±0.7	0.847±0.022	0.963±0.059	225.5±3	349.9±2	127.2±2.6	11

2 New showers

The file with all individual meteor orbits of the new showers described in this article can be downloaded from the CMN download page:
`http://cmn.rgn.hr/downloads/downloads.html`

The orbital elements of showers discussed in this article are summarized in Table 1. Members of all showers discussed here were also detected through analysis of the IMO single station observation database.

The radiant plots (Figures 1–3) are grouped together to save space. The value of generic D-criterion (the mean value of $D_{SH}/2$, $D_H/2$ and D_D, with the additional constraint that all three have to be smaller than the preset limit, as described before) is coded in gray scale (in the electronic edition they are color-coded). Additionally, radiants that belong to known showers active in the same period as the new ones are indicated by larger circles.

2.1 15 Aquariids (548 FAQ)

39 meteors spread over 16 days are associated with this shower. After a slow rise in the first week, the number of orbits per day is about 2.4. Apart from clearly evident daily motion, the radiant plot also shows a concentration of individual meteors around the mean radiant position. Moreover, 23 meteors are observed in only 5 degrees of solar longitude (109–114°). Active July 5 to 23, the mean corresponding to July 15.

2.2 49 Andromedids (549 FAN)

35 meteors spread over 14 days are associated with this shower. The number of orbits per day is more or less constant with about 2.5 orbits per day. Apart from clearly evident daily motion, radiant plot does not reveal any structure. Active July 10 to 25, the mean corresponding to July 17.

The shower 411 CAN is nearby, but mean orbits differ a lot, with a D_{SH} of 0.59, so they are clearly two different showers.

A possible parent body for this shower is comet C/2001 W2 (BATTERS). A D_{SH} of 0.14 indicates that the possibility of connection between 549 FAN and this comet is quite real. Earth MOID of 0.15 AU is rather large, but angular orbital elements of the comet and 549 FAN are very similar (Table 2). Thus, there is clearly a need for further analysis of this comet and its relation to 549 FAN.

Table 2 – Comparison of orbital elements of 49 Andromedids (mean orbit) and the orbit of comet C/2001 W2 (BATTERS).

parameter	549 FAN	C/2001 W2
q	0.918	1.051
e	0.925	0.941
ω	143.1	142.1
Ω	114.0	113.4
i	118.2	115.9
D_{SH}	0.141	
MOID		0.15

2.3 κ Cassiopeiids (550 KPC)

16 meteors spread over 8 days are associated with this shower. The number of orbits per day is more or less constant with about 2 orbits per day. Radiant plot does not reveal any structure, even the daily motion is not noticeable, mainly due to the short duration of the shower and large dispersion of the radiant. Active July 17 to 25, the mean corresponding to July 22.

2.4 47 Andromedids (551 FSA)

36 meteors spread over 15 days are associated with this shower. The average number of orbits per day is 2.4, but the actual number of orbits per day sharply increases just before the mean solar longitude, and falls to about average after that. Apart from clearly evident daily motion, radiant plot does not reveal any structure. Active August 3 to 19, the mean corresponding to August 11.

The shower 534 FOA is nearby, but mean orbits differ by $D_{SH} = 0.33$ so they are clearly different showers.

2.5 δ Perseids (553 DPE)

35 meteors spread over 17 days are associated with this shower. The average number of orbits per day is about 2.0, slowly increasing towards the mean solar longitude and declining in the same way afterwards. Apart from clearly evident daily motion, radiant plot does not reveal any structure. Active September 2 to 20, the mean corresponding to September 11.

208 SPE is nearby, but mean orbits differ by $D_{SH} = 0.53$, too much for them to be the same shower.

2.6 α Perseids (554 APE)

31 meteors spread over 12 days are associated with this shower. The mean number of orbits per day is about 2.6, with a slight increase around the mean solar longitude. Apart from clearly evident daily motion, radiant plot does not reveal any structure. Active September 8 to 21, the mean corresponding to September 14.

Two other showers are nearby, 208 SPE with $D_{SH} = 0.35$ and 553 DPE, also with $D_{SH} = 0.35$.

2.7 October γ Camelopardalids (555 OCP)

16 meteors spread over 8 days are associated with this shower. The number of orbits per day is about 2.0. Apart from clearly evident daily motion, radiant plot does not reveal any structure. Active October 2 to 10, the mean corresponding to October 5.

An interesting fact is that the orbit of this shower is almost perpendicular to the plane of the ecliptic.

2.8 ϕ Taurids (556 PTA)

22 meteors spread over 12 days are associated with this shower. The number of orbits per day is about 1.8. Apart from clearly evident daily motion, radiant plot is quite compact. Active September 30 to October 12, the mean corresponding to October 6.

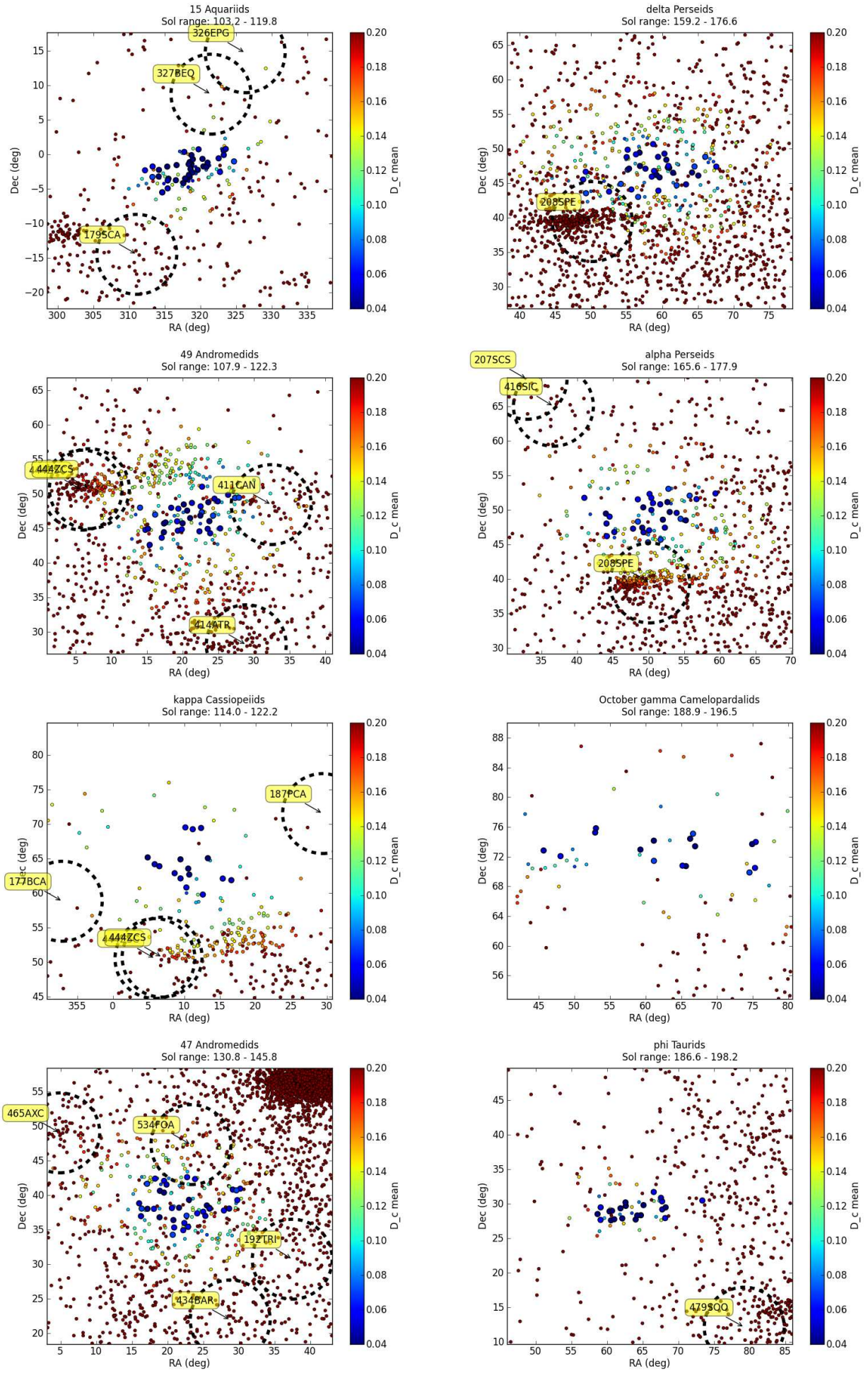

Figure 1 – Radiant plots of showers 548 FAQ to 556 PTA.

2.9 64 Draconids (557 SFD)

37 meteors spread over 16 days are associated with this shower. The number of orbits per day is about 2.3. Apart from clearly evident daily motion, radiant plot does not reveal any structure. Active October 21 to November 6, the mean corresponding to October 30.

The radiants of 525 ICY and 83 OCG are nearby, but at a distance of about 15° still too far away to consider them parts of the same shower.

2.10 27 Monocerotids (558 TSM)

29 meteors spread over 14 days are associated with this shower. The number of orbits per day is about 2.1. Apart from clearly evident daily motion, radiant plot does not reveal any structure. Active October 28 to November 11, the mean corresponding to November 4.

2.11 β Canis Majorids (559 MCB)

20 meteors spread over 9 days are associated with this shower. The number of orbits per day is more or less constant with about 2.2 orbits per day. Apart from clearly evident daily motion, radiant plot does not reveal any structure. Active November 16 to 25, the mean corresponding to November 19.

Despite the radiant plot suggesting a similarity between this shower and 394 ACA, the resulting D_{SH} of 0.37 is too large to consider them as parts of the same shower. 394 ACA was not found by our search, but this can be explained by the fact that 394 ACA is a radar shower.

2.12 17 Sextantids (560 SES)

39 meteors spread over 20 days are associated with this shower. The number of orbits per day is about 2.0. Apart from clearly evident daily motion, radiant plot does not reveal any structure. Active December 3 to 23, the mean corresponding to December 14.

2.13 6 Sextantids (561 SSX)

44 meteors spread over 22 days are associated with this shower. The number of orbits per day is about 2.0, being strongest around the mean solar longitude, with a gradual decrease towards smaller and larger $\lambda_\odot$. Apart from clearly evident daily motion, radiant plot does not reveal any structure. Active December 3 to 25, the mean corresponding to December 14. The meteors of this shower are very bright, with a mean magnitude of about -1.8.

This shower may be related to the previous one, 560 SES. The D_{SH} of 0.39 excludes the possibility of them being identical, but they may be part of a group of related showers.

2.14 13 Comae Berenicids (562 BCT)

50 meteors spread over 20 days are associated with this shower. The mean number of orbits per day is about 2.5, with increasing activity a few days after the mean solar longitude. The daily motion is evident in the radiant plot, as is the concentration of orbits around the mean $\lambda_\odot$ of the activity period. Active December 8 to 27, the mean corresponding to December 17.

20 COM is nearby in RA, DEC and $\lambda_\odot$, but clearly different, with a D_{SH} of 1.2.

2.15 December ω Ursae Majorids (563 DOU)

50 meteors spread over 11 days are associated with this shower. The mean number of orbits per day is about 4.5, thus making this shower about two times as active as the others reported here. Apart from clearly evident daily motion, radiant plot does not reveal any structure. Active December 15 to 27, the mean corresponding to December 21. The meteors of this shower are very bright, with a mean magnitude of about -1.7.

2.16 61 Ursae Majorids (564 SUM)

33 meteors spread over 14 days are associated with this shower. The number of orbits per day is about 2.4. The radiant plot is rather scattered, with a moderate elongation due to the daily motion. Active December 22 to January 4, the mean corresponding to December 27.

2.17 59 Ursae Majorids (565 FUM)

36 meteors spread over 14 days are associated with this shower. The number of orbits per day is about 2.6, being moderately stronger at the beginning of the activity period, with a smooth decrease towards its end. Apart from clearly evident daily motion, radiant plot does not reveal any structure. Active December 23 to January 5, the mean corresponding to December 30.

2.18 5 Comae Berenicids (566 BCF)

36 meteors spread over 16 days are associated with this shower. The number of orbits per day is about 2.3. The radiant plot is diffuse, and the daily motion is not evident. From the radiant plot the possibility can be seen that there may be two branches, but additional analysis should be done to check this hypothesis since it is not conclusive from the radiant plot only. Active December 23 to January 8, the mean corresponding to December 30.

20 COM is nearby in RA, DEC and $\lambda_\odot$, but clearly different, with a D_{SH} of 0.86.

2.19 ξ Hydrids (567 XHY)

26 meteors spread over 10 days are associated with this shower. The number of orbits per day is about 2.6. Apart from clearly evident daily motion, radiant plot indicates slow build-up of activity with time. Active December 30 to January 9, the mean corresponding to January 4.

2.20 14 Canum Venaticids (568 FCV)

17 meteors spread over 7 days are associated with this shower. The number of orbits per day is about 2.4. The daily motion is clearly evident in the radiant plot with an indication of larger activity around the mean solar longitude of the shower. Active January 26 to February 1, the mean corresponding to January 29.

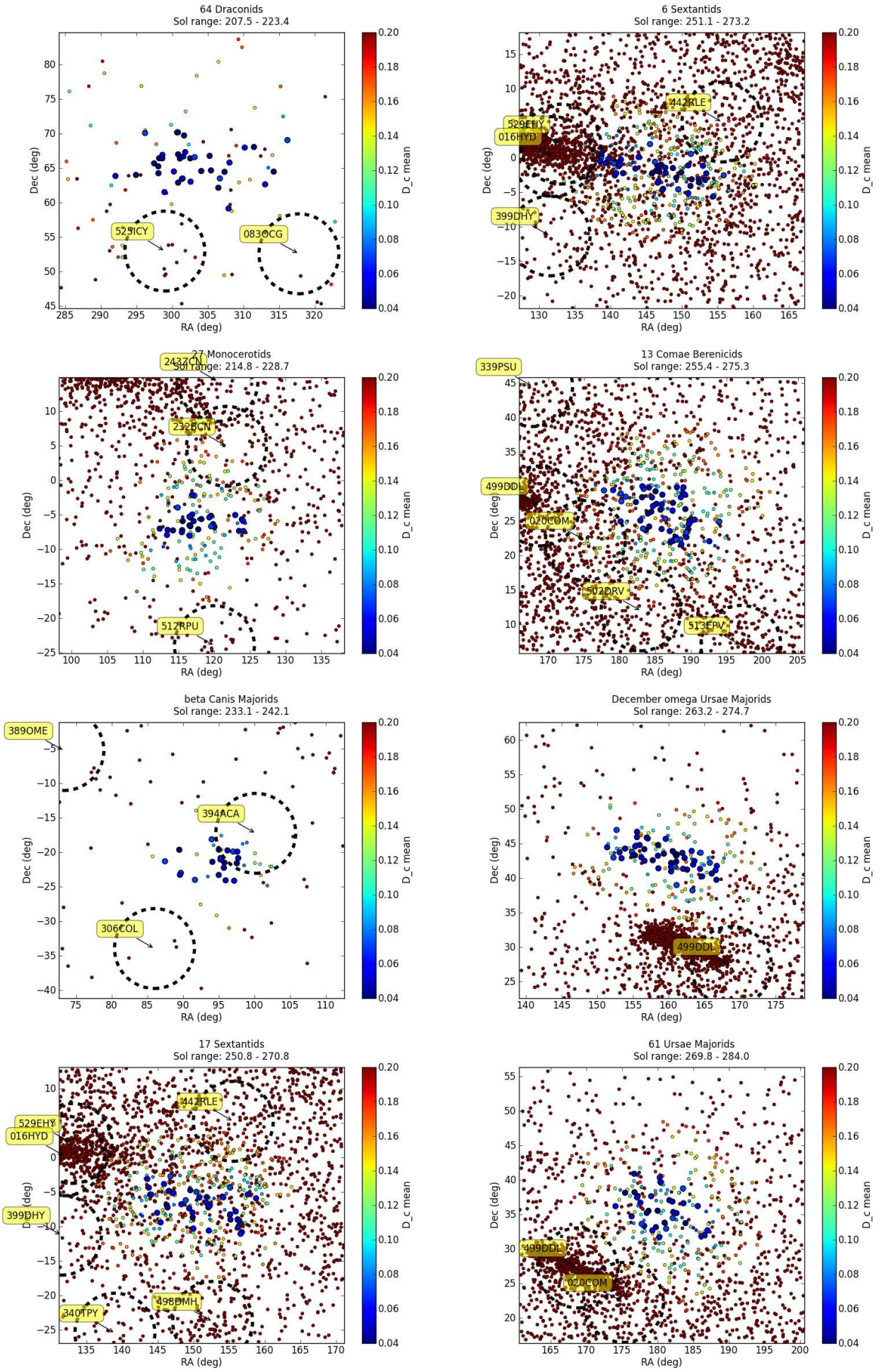

Figure 2 – Radiant plots of showers 557 SFD to 564 SUM.

2.21 *o* Hydrids (569 OHY)

29 meteors spread over 13 days are associated with this shower. The number of orbits per day is about 2.2. Apart from clearly evident daily motion, radiant plot does not reveal any structure. Active January 22 to February 5, the mean corresponding to January 29.

The 316 BHD radiant is about 15° from the 569 OHY radiant, but possible connections cannot be checked as there are no orbital data for 316 BHD in the IAU MDC database.

2.22 February β Herculids (570 FBH)

24 meteors spread over 10 days are associated with this shower. The number of orbits per day is about 2.4. The radiant plot is concentrated but apart from clearly evident daily motion, it does not reveal any structure. Active January 28 to February 7, the mean corresponding to February 3.

2.23 26 Bootids (571 TSB)

10 meteors spread over 4 days are associated with this shower. The number of orbits per day is about 2.5. The radiant plot is quite concentrated and does not reveal any structure. Active March 2 to 6, the mean corresponding to March 4. The members of this shower are very bright, with a mean magnitude of about −1.6.

2.24 21 Herculids (572 TOH)

11 meteors spread over 5 days are associated with this shower. The number of orbits per day is about 2.2. The radiant plot does not reveal any structure. Active March 8 to 13, the mean corresponding to March 10.

Acknowledgements

Our acknowledgments go to all members of the Croatian Meteor Network. In alphabetical order of first name: Alan Pevec, Aleksandar Borojević, Aleksandar Merlak, Alen Žižak, Berislav Bračun, Dalibor Brdarić, Damir Matković, Damir Šegon, Dario Klarić, David Gostinski, Dejan Kalebić, Denis Štogl, Denis Vida, Dorian Božićević, Filip Lolić, Filip Novoselnik, Gloryan Grabner, Goran Ljaljić, Ivica Ćiković, Ivica Pletikosa, Janko Mravik, Josip Belas, Korado Korlević, Krunoslav Vardijan, Luka Osokruš, Maja Crnić, Mark Sylvester, Mirjana Malarić, Reiner Stoos, Saša Švagelj, Sonja Janeković, Tomislav Sorić, VSA group 2007, Zvonko Prihoda, Željko Andreić, Željko Arnautović, Željko Krulić.

This work was partially supported by the Ministry of Science, Education and Sports of the Republic of Croatia, Faculty of Mining, Geology and Petroleum Engineering, University of Zagreb, Višnjan Science and Education Center and by private funds of CMN members.

References

Drummond J. D. (1981). "A test of comet and meteor shower associations". *Icarus*, **45**, 545–553.

International Meteor Organization (1993-2012). "IMO video meteor database". `http://www.imonet.org/database.html` .

Jopek T. J. (1993). "Remarks on the meteor orbital similarity D-criterion". *Icarus*, **106**, 603–607.

Southworth R. B. and Hawkins G. S. (1963). "Statistics of meteor streams". *Smithsonian Contr. Astrophys.*, **7**, 261–285.

Šegon D., Gural P., Andreić Ž., Skokić I., Korlević K., Vida D., and Novoselnik F. (2014a). "New showers from parent body search across several video meteor databases". *WGN, Journal of the IMO*, **42:2**, 57–64.

Šegon D., Gural P., Andreić Ž., Skokić I., Korlević K., Vida D., and Novoselnik F. (2014b). "A parent body search across several video meteor data bases". In Jopek T. J., Rietmeijer F. J. M., Watanabe J., and Williams I. P., editors, *Proceedings of the Meteoroids 2013 Conference, Aug. 26-30, 2013, A. M. University, Poznań, Poland*. Adam Mickiewicz Univ. Press, pages 251–262.

Handling Editor: David Asher

This paper has been typeset from a LaTeX file prepared by the authors.

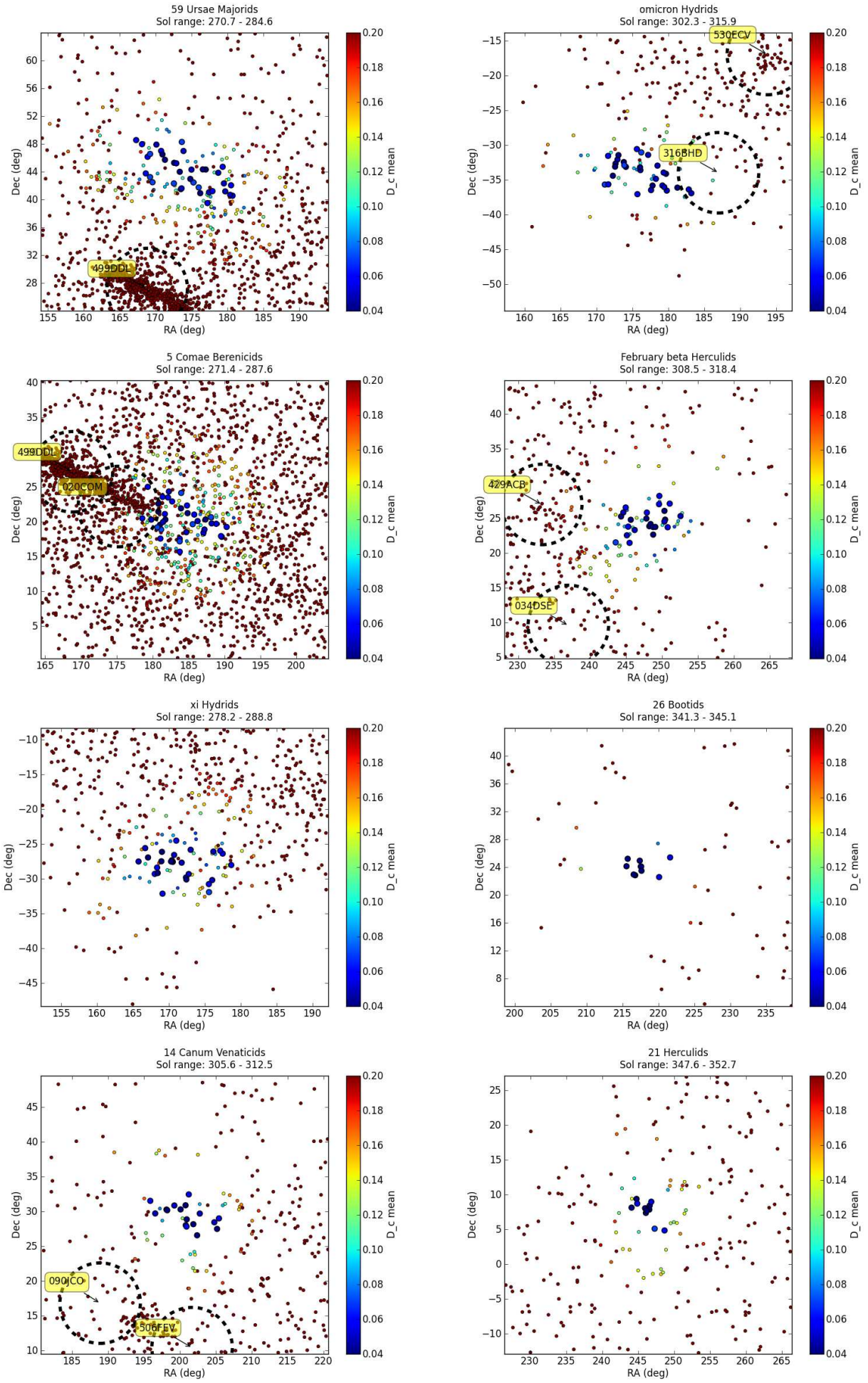

Figure 3 – Radiant plots of showers 565 FUM to 572 TOH.

Camelopardalids (IAU#451) from comet 209P/LINEAR

Peter Jenniskens[1]

Since shortly after the comet's discovery in 2004, the close encounter of comet 209P/LINEAR with Earth on 2014 May 29 was highly anticipated as an opportunity to measure past activity of the comet. Only five days earlier, Earth would encounter ejecta from the 18th, 19th and 20th centuries. The outburst was observed from 7–8 km altitude during a SETI Institute sponsored airborne observing campaign. 21 Camelopardalids were detected, for an equivalent peak ZHR $\sim 13 \pm 4$ /h. The meteors were faint, with high magnitude distribution index $\chi = 3.7 \pm 0.5$ in the -1 to $+5$ magnitude range, which translates to a differential mass distribution index of $s = 2.42 \pm 0.15$ (0.003–4 g) and a differential size distribution index of $\alpha = 5.3 \pm 0.4$ (0.2–2 cm). The meteors fragmented excessively towards the end of their trajectory. Twenty trajectories were triangulated in ground-based observations, showing a compact geocentric radiant at RA = $119\overset{\circ}{.}9 \pm 5\overset{\circ}{.}3$, Dec = $+78\overset{\circ}{.}2 \pm 0\overset{\circ}{.}9$, with speed $V_g = 14.9 \pm 0.7$ km/s, close to the predicted position. Light curves were U-shaped, with peak luminosity at 88 km altitude, where a wake faded in 1.08 ± 0.17s (1/e). Activity was of relatively long duration (5-h FWHM). It remains unclear when this dust was ejected.

Received 2014 June 11

1 Introduction

Comet 209P/LINEAR is a weakly active Jupiter Family comet with an orbital period of 5.02 years. Discovered in 2004, it approached Earth to only 0.0554 AU on 2014 May 29, now the 9th closest encounter of a comet to Earth on record and the closest since comet IRAS-Araki-Alcock in 1983. 2014 was the first year the comet orbit evolved to passing close to Earth's orbit, and it will keep doing so until the return of 2044. Other such weakly active comets had past disruptions that created some of our most significant meteor showers, including the alpha Capricornids, kappa Cygnids, Quadrantids and Geminids (Jenniskens, 2008).

Shortly after its discovery, Esko Lyytinen and I realized that, just five days earlier, Earth would pass close to some 19th and 20th century dust trails, assuming that the comet was active in the past (Table 6j of Jenniskens, 2006). Vaubaillon (2012) confirmed that many of the 18th, 19th and early 20th century dust trails would be in Earth's path on 2014 May 24 around 07^h UT, and piled up in a narrow region of nodes. Ye & Wiegert (2014) examined the comet activity in 2009 and concluded that the shower would be broader than predicted by Vaubaillon (2012), peaking slightly earlier, and dominated by bright meteors (particles larger than 1 mm in size, or visual magnitude $M_v < +5.4$ magnitude).

The new meteor shower would be mainly visible from the United States and southern parts of Canada. The expected level of activity was unknown, if any, because there were no prior encounters with the dust ejected by comet 209P/LINEAR. If the comet was not active in the past, there would be no new shower at all. Assuming the activity was the same as today, both Vaubaillon (2012) and Ye & Wiegert (2014) put the expected peak rate within a factor of two from ZHR = 200/h.

[1]SETI Institute, 189 N. Bernardo Ave., Suite 100, Mountain View, CA 94043, USA. Email: petrus.m.jenniskens@nasa.gov

IMO bibcode WGN-423-jenniskens-camelopardalids
NASA-ADS bibcode 2014JIMO...42...98J

The hope that some activity would be observed increased when a weak shower was detected in early May CAMS and SonotaCo video observations (Rudawska & Jenniskens, 2014). The period of activity was later extended to cover the time of the expected outburst (Šegon et al., 2014). This shower was called the Camelopardalids (IAU#451, CAM). That weak activity implied the comet was active in the past, but it remained unknown if that was during the timeframe relevant for the May 24 encounter.

The upcoming activity in 2014, if any, would provide insight into the comet's activity in the centuries before its discovery. Because of the potential that significant dust might be released in the past, the shower was highly anticipated (Jenniskens & Lyytinen, 2014; Rao, 2014).

2 Observing Campaign

California was well positioned for viewing the anticipated shower. If the shower would indeed be skewed towards brighter meteors, then this would not be an easy radar target and flux measurements were best made by optical cameras from the air. The large surface area near the horizon, combined with low extinction, would result in a higher rate of meteors per square degree at the low 5–10° elevations (Gural & Jenniskens, 2000).

The SETI Institute board of trustees chartered a Beechcraft King Air 90 aircraft out of Palo Alto airport to take a team of researchers to 6–8 km altitude for best viewing of the shower. With only 36 hours of advance notice that the mission would proceed, we used the event to practice the rapid response to a possible future announced asteroid impact. Because of that, a mission patch with no date was designed (Figure 1) and team member Ron Dantowitz of Dexter Southfield Schools flew out to California from Brookline, Massachusetts. Local team members included Mike Koop, Jim Albers and Alan Dunton.

Five intensified cameras were deployed in the main cabin, three Gen II of type XX1332 and two of type MX-9916/UV, all providing a star limiting magnitude of +6.9 and a field of view of about $40° \times 30°$, aimed

Figure 1 – The SETI Institute airborne observing campaign to study the new shower from 209P/LINEAR. From left to right: Ron Dantowitz, Peter Jenniskens, Mike Koop and Jim Albers. Right: flight path out of Palo Alto, California. For more information, see the mission website at `http://meteor.seti.org`.

at $\sim 16°$ elevation (Gural & Jenniskens, 2000). During the flight, we performed real-time flux measurements by viewing three of the cameras, a fourth person (Alan) making notes of the count every minute. Results were posted shortly after the flight results were announced the next morning. In addition, Ron fielded two Lumenera 2-1R Silicon based CCD cameras for imaging (resulting in 72 764 spatial images) and spectroscopy (5 200 spectroscopic images).

The mission was supported by ground-based low-light level video observations. Weather permitting, the 60-videocamera CAMS network in the San Francisco Bay Area would measure trajectories, light curves, and pre-atmospheric orbits, and also obtain meteor spectra from the station in Sunnyvale (Jenniskens et al., 2011). In addition, six single-CAMS cameras operated in Brentwood, Walnut Creek, San Mateo College, and Foresthill (administered by Dave Samuels). In the BeNeLux, a 30-camera single-CAMS network was in operation (administered by Carl Johannink), which covered the early and late parts of the meteor shower profile. On the Mid-Atlantic East Coast, Pete Gural administered a 7-camera single-CAMS network and operated one intensified camera at Mt. Airy, MD, of the same type (XX1332, 50mm $f/1.2$ lens) as deployed airborne, set up with $39° \times 49°$ field of view (5.3 arcmin/pixel) pointed to elevation 56° and azimuth 246°.

3 Results

The airborne observations.

Quite to my relief, the shower did show. The wheels left the runway right on time at $05^{h}30^{m}$ UT. In the next half hour, the aircraft climbed to altitude and away from city light and haze. Observations with the cameras viewing west towards the ocean were started at $06^{h}00^{m}$ UT. Eastwards looking cameras were initially hampered by city lights and recorded data starting at

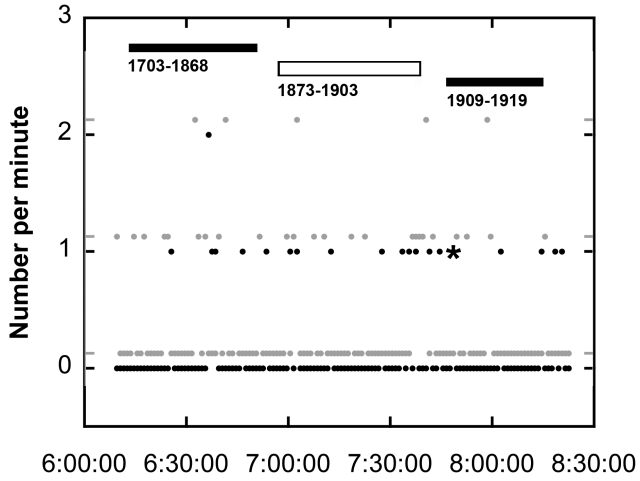

Figure 2 – Count per minute of Camelopardalids from altitude, with sporadic count in gray and offset. Trails: Vaubaillon (2012).

$06^{h}17^{m}$ UT. The aircraft followed a flight path towards the shower radiant (Figure 1). At $07^{h}22^{m}$–24^{m} UT, the aircraft reached the furthest point and turned back to Palo Alto. The sky was mostly clear above the wing tip throughout the flight, but occasionally clouds traversed the 5–10° elevation band. Observations were made until $08^{h}23^{m}$ UT, with the eastward looking cameras becoming much brighter from city lights after $08^{h}18^{m}$ UT.

The observing period covered the full range of encounter times of dust trails calculated by Vaubaillon (2012), who found that the older 17th and early 18th century dust trails tended to be encountered around $06^{h}30^{m}$ UT, while the more recent 1909–1914 trails were expected to peak around $08^{h}00^{m}$ UT (Figure 2).

The occurrence of Camelopardalids is marked in Figure 2. The rate increased gradually during the night, and peaked when crossing the relatively recent 1903 dust trail. The first magnitude +5 Camelopardalid was seen at $06^{h}25^{m}42^{s}$ UT, moving at a $\sim 20°$ angle to the

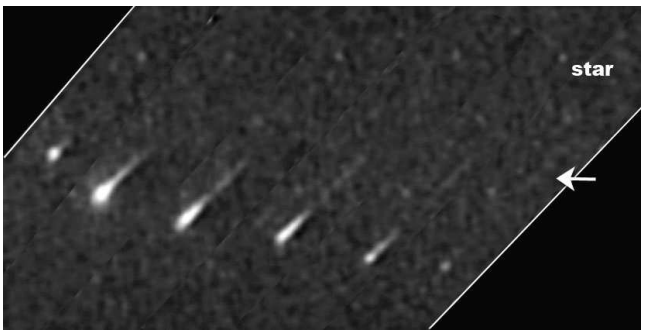

Figure 3 – The 2014 May 24, $07^h48^m12^s.5$–$14^s.9$ UT Camelopardalid in Corvus (compilation of frames at $07^h48^m12^s.5$, $13^s.0$, $13^s.5$, $13^s.7$, $14^s.0$, and $14^s.9$). The arrow points towards the persistent emission.

horizon from the North, gliding through the air with low angular velocity. All video tapes were later viewed again and meteors plotted on gnomonic star charts to confirm radiant association and determine the meteor magnitude relative to the background stars. A total of 21 Camelopardalids and 38 other meteors were detected in the two hours of observations.

Few meteors appeared as low as 5–10°. The star limiting magnitude was good near the horizon, based on counts in area #23 in Corvus. At 11 km altitude, the nominal extinction is less than 0.1 magnitude at 10° elevation and 0.3 magnitude at 5° elevation, about six times lower than on the ground (Gural & Jenniskens, 2000). The fact that we were flying at only 6–8 km did not affect the conditions much. Distant clouds were a problem in some cameras, but a clear stretch from 07^h24^m to 07^h54^m UT in the westward looking cameras only produced one low Camelopardalid, also the brightest of the night (Figure 3). We carefully examined for slow moving meteors, but found no other in the 5–10° band.

The only explanation is that the magnitude distribution index (χ) of the stream was rather high, contrary to expectations. Indeed, most Camelopardalids captured on video had a low apparent visual magnitude. From +5 down brighter magnitudes, we captured: 7, 10, 1, 1, 1, and 1 Camelopardalid, respectively. In contrast, we captured: 6, 10, 13, 2, and 2 for all other meteors. After correction for camera detection efficiency, the calculated $\chi \sim 3.8 \pm 0.8$.

The bright +0.2 magnitude Camelopardalid at $07^h48^m13^s$ UT was distinctly elongated towards the end (Figure 3) and left a persistent emission at peak brightness (altitude $\sim$ 88 km based on triangulated meteors, see below). This emission is orange in color in video by Prof. Peter C. Slansky of the Munich Academy of Television and Film (see front cover), from which the derived 1/e decay time is 1.08 ± 0.17 s (during 3.4 s). The elongation of the meteoroid and an abrupt velocity change past peak brightness (Figure 3) is due to a flare-less whole-scale breakup event into small particles with high surface-to-mass ratio. Dust collection efforts in the upper atmosphere are ongoing, in the hope that this debris may stand out from the normal meteoric influx, taking many days or weeks to settle.

Ground-based observations.

CAMS station operators Jim Albers (Sunnyvale) and Bryant Grigsby (Lick Observatory) quickly made raw data available to be able to confirm the shower radiant. The first Camelopardalid meteor was captured by the CAMS network in the night before the peak, at 04^h48^m UT on May 23. Later that day, CAMS@BeNeLux network administrator Carl Johannink reported that this network captured three more. Most meteors were detected on May 24 by the California network, including one at $06^h41^m13^s$ UT by the SingleCAMS camera stations 216 (Brentwood), 214 (Forrest Hill) and 218 (Walnut Creek), administered by Dave Samuels (Figure 3). Sadly, intermittent clouds hampered observations in California right around the peak between 05^h12^m and 09^h00^m UT. Fourteen trajectories were measured before and after the peak. No spectra were obtained. The CAMS@Mid-Atlantic network had clear weather with magnitude +5.8 skies and administrator Peter Gural calculated one Camelopardalid trajectory. Later that day, the CAMS@BeNeLux network captured one final late Camelopardalid at 22^h27^m UT.

Table 1 summarizes the results of the 20 trajectories, including some that were not so precisely measured and would normally be rejected. Twelve cluster tightly around geocentric radiant RA = $119^\circ.9 \pm 5^\circ.3$, Dec = $+78^\circ.2 \pm 0^\circ.9$, with speed V_g = 14.9 ± 0.7 km/s. The predicted radiant position from dust of comet 209P/LINEAR was RA = 125°, Dec = +78°, with speed $V_g = 15.8$ km/s (Jenniskens, 2006), in good agreement.

Figure 4 shows the distribution of radiant positions measured by all CAMS networks on May 23–24. The Camelopardalids (CAM) stand out well from other shower activity (including the eta Aquariids (#31), the Scorpiid-Sagittariid Complex (#163), chi Librids (#275), and zeta Puppids (#300)) and from the apex and antihelion sporadic sources.

Ten Camelopardalids showed an U-shaped light curve, with a hint of an end flare due to the abundant fragmentation ('A' and 'C' in Figure 5). Peak brightness occurred at around 88 km altitude, near the upper range of other meteors with 19 km/s entry speed (Figure 5). A total of 13 out of 20 meteors (65%) have a light curve peaking early ($F < 0.50$, Table 1), which has been interpreted as typical for fragile meteoroids (Murray et al., 2000). One late bright Camelopardalid showed a more gradual rise ('D'), indicative of a more sturdy meteoroid (Figure 5).

Ten meteor lightcurves were more sharply peaked (V-shape), with peak brightness lower in the atmosphere ('B' and cross in Figure 5). These short tracks produced poor trajectory solutions, as a result of which many have outlaying radiant positions. Ignoring these in Figure 4 (gray symbols) leaves only radiant positions at the compact radiant. It is not clear whether the low altitudes are a physical phenomenon of the meteors, or a problem in the trajectory solution. Other 19 km/s showers also have such solutions in CAMS data.

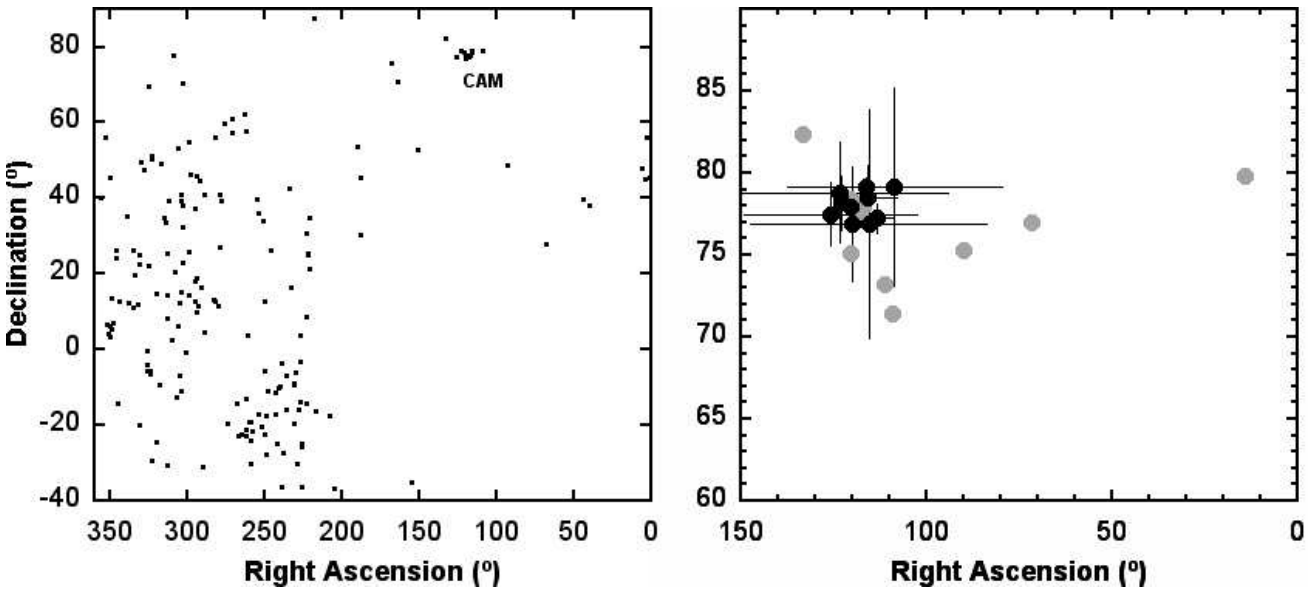

Figure 4 – CAMS-measured geocentric radiant positions on 2014 May 23 and 24. Gray: Meteors with short V-shaped lightcurves.

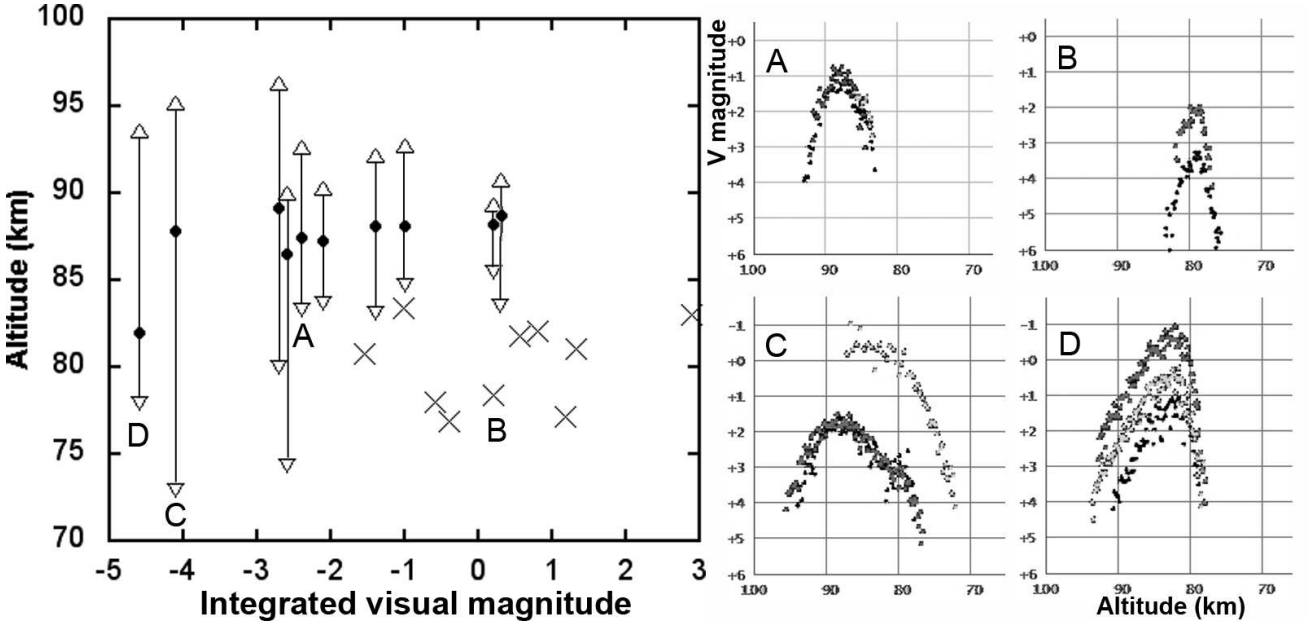

Figure 5 – Example meteor lightcurves and altitude range (• and × mark peak brightness) plotted as a function of the integrated meteor brightness. A: Typical case at $04^{h}41^{m}02^{s}$ UT; B: Likely incorrect, sharply peaked result at $05^{h}15^{m}59^{s}$ UT; C: Single-CAMS result at $06^{h}41^{m}13^{s}$ UT; D: Large meteoroid at $11^{h}34^{m}14^{s}$ UT.

Many of the multi-station Camelopardalids are relatively bright, peaking at +1 and +2 magnitude, but that is an effect of the detection probability of the network. Based on all non-shower (sporadic) meteors triangulated until 2013 March, we have detection probabilities from magnitude +5 down brighter magnitudes: 4e-5, 0.0018, 0.018, 0.080, 0.27, 0.64, 0.98, 1.00, 1.00,... and sporadic $\chi_s = 3.24$. Based on this correction, the Camelopardalids had $\chi = 3.8 \pm 0.4$.

The ground-based intensified camera operated by Pete Gural from a location in Mt. Airy in Maryland, captured 25 Camelopardalids in the 6-h period from $02^{h}00^{m}$ to $08^{h}00^{m}$ UT. The final ten minutes were affected by dew on the lens. The meteors were extracted using Meteor Scan and a new single-track radiant-association algorithm was used to confirm the shower association based on direction and angular velocity. The apparent magnitude distribution from +5 down brighter magnitudes: 11, 10, 4, 0, from which the magnitude distribution index $\chi \sim 3.2$. Nine more single station Camelopardalids were captured in the CAMS@Mid-Atlantic network, all of +3 ($N = 5$) and +4 magnitude. Because the meteors were so faint, the range loss was significant enough for these meteors not to be detected at the other sites, resulting in few two-station coincident observations for triangulation.

Because of clouds, meteor rates are difficult to evaluate from the ground-based CAMS data in California. From the airborne Camelopardalids observed above 15° elevation, we have an equivalent ZHR = 9.9 ± 3.7 at

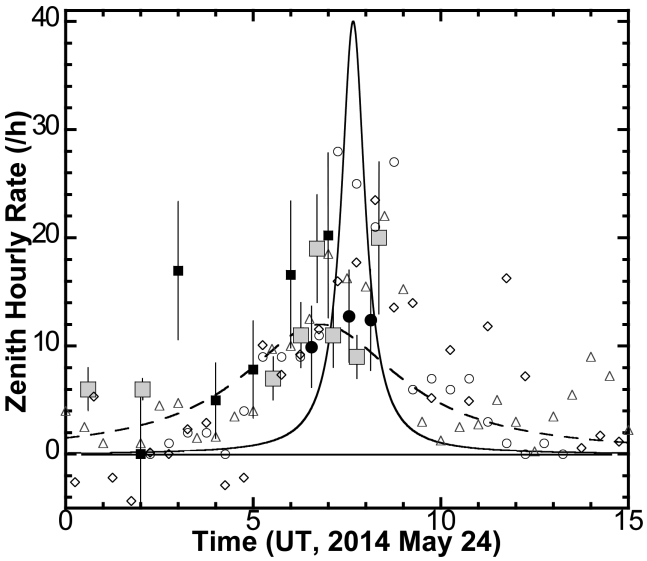

Figure 6 – Activity curve. • = airborne video; ■ = ground-based intensified video; ■ = IMO visual (International Meteor Organization, 2014); open symbols are Radio forward meteor scatter data by Hirofumi Sugimoto (Japan, ○), and scaled to match: Jeff Brower (British Columbia, ◇), and Peter Bus (△). Predictions are those by Vaubaillon (solid line) and Ye & Wiegert (dashed line).

06^h33^m UT, 12.8 ± 4.3 at 07^h33^m UT, and 12.4 ± 4.7 at 08^h08^m UT, but systematic errors may be higher than the random errors. These rates are shown as solid circles in Figure 6. The Mid-Atlantic CAMS stations were clear. The rate of Camelopardalids observed by the Mt. Airy camera translates into the equivalent ZHR values shown as black squares in Figure 6.

The results are compared to radio forward-meteor-scatter counts provided by Jeff Brower of British Columbia and Peter Bus of the Netherlands (Bus, 2014), which were scaled to match the rates from video data. Independently calibrated are similar data published online by Hirofumi Sugimoto from Japan (○), and the IMO calculated near-real time ZHR values (International Meteor Organization, 2014) from visual observations of the shower (open squares, data as of June 9). The graph also shows the predictions by Vaubaillon (2012) as a solid line and by Ye & Wiegert (2014) as a dashed line, both with rates scaled to match the observed profile, a factor 20 less than predicted.

4 Discussion

There is no doubt that we encountered the dust of comet 209P/LINEAR. All prediction models correctly calculated the general time of when this dust was encountered. This is the first meteor outburst observed from ejecta of comet 209P/LINEAR.

That said, it is not so clear to me when this dust was ejected. The steep magnitude distribution index is very interesting, because it means that large particles were lost by processes other than collisions (Jenniskens, 2006). Ye & Wiegert (2014) correctly predicted the 5-h duration of the shower, but perhaps not based on the correct physics of dust ejection. They assumed a dust differential size distribution index $\alpha = 2.6$, based on the large-grain size distribution of dust ejected by 1P/Halley. A relatively long section of the dust trails was integrated, when plotting up the dust density at Earth. Moreover, the dynamics of dust delivery does not reflect their result that particles arriving at Earth would be skewed strongly to larger particles and be mostly larger than 1 mm ($M_v < +5.4$), and the resulting shower dominated by bright meteors. This would suggest a collisionally relaxed $\chi \sim 1.85$ (Jenniskens, 2006).

The observed $\chi = 3.7 \pm 0.5$ translates to a differential mass distribution index $s = 2.42 \pm 0.15$ and size index $\alpha = 5.3 \pm 0.4$. The abundance of faint meteors resulted in an unexpected strong detection by the CMOR radar, which is sensitive predominantly to the brightest underdense echoes of +6 and +7 magnitude (Brown, 2014).

Such a high magnitude distribution index is not unusual. It was also a feature of past Draconid outbursts from hyperactive comet 21P/Giacobini-Zinner ejecta in 1933 ($\chi = 3.6$) and 1946 ($\chi = 3.2$; Jenniskens, 2006). In that case, I suspect that the steep distribution comes from particle ejection being driven by CO_2 outgassing, so that the grains still contained water ice. When that water ice evaporated, the larger grains might have fallen apart into smaller grains. CO_2-driven outgassing would be hard to understand for a weakly active comet like 209P/LINEAR, but ice-laden material could be released in a fragmentation event of the comet itself. Could the 2014 Camelopardalids be an echo of a comet disintegration event in the past? While that is not impossible, the observed 20 times weaker-than-expected rates even from the current weak activity may argue against this.

It is perhaps more likely that the comet was weakly active also in the 18th, 19th, and early 20th centuries. In that case, the steep distribution index could come from the meteoroids falling apart over time. Past crossings of old Leonid dust trails also seemed to show such lower-than-expected peak activity (Jenniskens, 2006). The observed activity is centered on the most recent dust trails according to the times calculated by Vaubaillon (2012). Perhaps, these fragile cometary grains disappear over time by falling apart into finer dust due to thermal or centrifugal stresses. If so, the fading is rapid, with a 1/e timescale of only 30–50 years, assuming an initial dust density equivalent to ZHR = 100–400 in 2014. Are we seeing the accumulated effect of many centuries of fragile cometary meteoroids fading into memory? This should be modeled to see if it can explain the broader than expected shower in the model by Vaubaillon (2003).

Or are simply the particle ejection conditions different than assumed? Were the ejected particles small to begin with? Could ejection conditions have put the small particles preferentially in Earth's path, instead of the large particles? These questions may be answered soon. The comet itself was well observed in this encounter and will provide more insight into the conditions of the present day dust ejection.

Date 2014	Time (UT)	$\lambda_\odot$ (°)	$RA_\infty^\dagger$ (°)	Dec_∞ (°)	V_∞ (km/s)	a_1 (km)	a_2 (/s)	H_b (km)	H_e (km)	M_v (mag)	ΣM_v (mag)	m (g)	F	††	Q (°)	ΔT (s)	Source CAMS
5/23	$04^h48^m17^s$	61.810	143.49	+74.15	17.39	0.00	0.17	84.7	78.1	+1.4	−1.6	0.3	0.63	V	33	0.52	C
			±0.14	±0.66	±0.25	±0.06	±0.08										
5/23	$21^h34^m44^s$	62.482	155.42	+82.55	21.74	1.12	1.12	86.5	77.7	+2.0	+0.7	0.03	0.78	V/U	5	0.55	(B)
			±0.62	±0.82	±0.73	±0.13	±0.16										
5/23	$23^h55^m58^s$	62.576	142.93	+82.42	16.85	0.04	0.17	81.4	76.8	+2.4	+1.2	0.02	0.33	V	66	0.36	B
			±0.59	±0.42	±0.22	±0.05	±0.10										
5/23	$23^h58^m18^s$	62.578	139.71	+81.89	18.80	0.31	0.03	91.2	83.2	+2.7	+0.2	0.05	0.28	U	13	0.56	B
			±0.13	±0.42	±0.88	±0.17	±1.56										
5/24	$04^h11^m21^s$	62.747	142.12	+77.06	18.14	0.02	0.20	92.2	83.1	+2.3	−1.4	0.2	0.45	U	19	0.69	C
			±0.44	±0.30	±0.15	±0.01	±0.15										
5/24	$04^h41^m02^s$	62.766	147.82	+77.49	19.08	0.03	4.75	92.6	83.3	+0.8	−2.4	0.5	0.54	U, fr	30	0.72	C
			±0.11	±0.32	±0.70	±0.02	±0.16										
5/24	$04^h41^m04^s$	62.766	145.16	+78.10	18.30	0.02	0.17	96.3	80.0	+0.2	−2.7	0.7	0.43	U, fr	30	1.25	C
			±0.12	±0.10	±0.10	±0.02	±0.07										
5/24	$05^h15^m59^s$	62.790	137.32	+83.37	14.28	0.00	0.01	83.5	82.0	+0.8	−1.0	0.15	0.11	V	15	0.15	(C)
			±0.78	±1.07	±0.29	±0.01	±0.10										
5/24	$05^h21^m27^s$	62.793	144.26	+79.46	17.77	0.25	0.55	92.7	84.7	+1.5	−1.0	0.15	0.57	U, fr	38	0.67	C
			±0.15	±0.13	±0.80	±0.08	±0.91										
5/24	$05^h45^m48^s$	62.810	277.21	+86.70	14.87	0.72	2.27	78.2	75.9	+1.4	−0.4	0.08	0.57	V	13	0.30	(C)
			±2.86	±3.18	±1.24	±0.15	±0.35										
5/24	$06^h41^m14^s$	62.847	151.29	+78.63	19.41	0.01	3.77	95.2	72.9	−0.4	−4.1	2.5	0.33	U, fr	10	2.09	sC
			±0.19	±0.66	±0.79	±0.25	±1.60										
5/24	$07^h43^m00^s$	62.888	129.91	+84.26	17.84	0.00*	0.00*	82.4	78.2	+3.7	+1.3	0.02	0.49	V	89	0.42	(M)
			±0.25	±0.28	±0.20	–.–	–.–										
5/24	$07^h51^m41^s$	62.894	151.99	+81.73	16.92	0.00*	0.00*	82.9	75.5	+2.0	−1.1	0.05	0.61	V, fr	27	0.72	C
			±0.16	±0.11	±0.05	–.–	–.–										
5/24	$08^h11^m43^s$	62.907	134.95	+78.56	16.37	0.00	6.39	90.3	83.7	+1.3	−2.1	0.4	0.45	U	42	0.75	(C)
			±7.45	±3.87	±3.64	±0.00	±2.23										
5/24	$08^h37^m07^s$	62.924	148.99	+82.30	18.79	0.01	3.12	90.0	74.3	+1.4	−2.7	0.7	0.36	wd, U	9	1.58	C
			±0.03	±0.12	±0.06	±0.00	±0.02										
5/24	$09^h25^m53^s$	62.957	144.44	+83.14	15.27	0.00	0.18	82.1	80.2	+2.1	+0.8	0.03	0.01	V	32	0.23	(C)
			±2.75	±2.15	±0.80	±0.05	±0.41										
5/24	$09^h37^m39^s$	62.964	280.25	+87.35	12.94	0.00	0.01	83.3	81.7	+4.4	+2.9	0.004	0.17	V	23	0.19	(C)
			±2.53	±1.34	±0.69	±0.01	±0.29										
5/24	$10^h01^m17^s$	62.980	128.86	+83.55	18.81	0.03	0.54	89.3	85.5	+1.9	+0.2	0.05	0.29	U	20	0.39	(C)
			±0.85	±1.38	±0.08	±0.03	±0.10										
5/24	$11^h34^m15^s$	63.042	119.17	+84.91	18.89	0.00	0.00*	93.7	77.9	−0.9	−4.6	4.0	0.73	sl, U	19	1.56	C
			±0.12	±0.07	±0.03	–.–	–.–										
5/24	$22^h27^m23^s$	63.478	162.34	+79.99	14.09	0.00	0.08	86.3	81.2	+2.7	+0.5	0.04	0.27	V	63	0.44	B
			±0.34	±0.28	±0.13	±0.02	±0.10										

Table 1 – Trajectory and lightcurve data of Camelopardalids from CAMS data. The a_1 and a_2 are parameters that describe the deceleration (Jenniskens et al., 2011); H_b, H_e are the beginning and end height of the meteor; M_v is the visual magnitude; ΣM_v is the integrated brightness, expressed in magnitude; m is the mass in grams; F is the relative position of the peak in the light curve (0 = begin, 1 = end); Q is the highest convergence angle of fitted planes to get the first trajectory solution; ΔT is the duration of the meteor. The source abbreviations are: C = CAMS network in California; sC = product of participating single CAMS stations; B = CAMS@BeNeLux; M = CAMS@MidAtlantic. A letter between brackets means that the measurement does not meet the normal CAMS precision criteria.

† Errors in Right Ascension are given as $\Delta RA \cos(Dec)$. a_1 and a_2 are defined in Jenniskens et al. (2011).

†† Notes: U = U-shaped; V = flare, V-shaped; fr = fragmentation (end flare), wd = wide; sl = slow rise.

Table 1 – (Continued)

Date 2014	Time (UT)	$\lambda_\odot$ (°)	RA_g (°)	Dec_g (°)	V_g (km/s)	q (AU)	$1/a$ (1/AU)	a (°)	i (°)	ω (°)	Ω (°)	Π (°)
5/23	$04^h48^m17^s$	61.810	120.3	+75.1	13.5	0.969	0.440	2.27	17.2	152.0	61.807	213.8
			±2.6	±0.8	±0.4	±0.006	±0.036		±0.4	±2.4	±0.002	±2.4
5/23	$21^h34^m44^s$	62.482	133.3	+82.4	18.7	0.970	0.222	4.50	24.9	154.8	62.478	217.3
			±12.6	±4.3	±0.9	±0.024	±0.127		±1.7	±7.5	±0.002	±7.5
5/23	$23^h55^m58^s$	62.576	117.1	+77.9	12.7	0.968	0.524	1.91	17.2	150.1	62.578	212.6
			±5.5	±4.6	±0.3	±0.007	±0.069		±1.3	±3.6	±0.001	±3.6
5/23	$23^h58^m18^s$	62.578	120.6	+78.4	15.2	0.966	0.387	2.58	20.0	151.8	62.578	214.4
			±7.6	±8.6	±1.2	±0.029	±0.081		±2.2	±12.0	±0.003	±12.1
5/24	$04^h11^m21^s$	62.747	115.9	+78.4	14.4	0.964	0.443	2.26	19.2	150.3	62.743	213.0
			±2.6	±2.1	±0.2	±0.005	±0.039		±0.7	±1.9	±0.001	±1.9
5/24	$04^h41^m02^s$	62.766	123.3	+78.8	15.6	0.968	0.368	2.72	20.5	152.4	62.762	215.2
			±9.5	±3.1	±0.8	±0.030	±0.112		±1.3	±10.1	±0.003	±10.1
5/24	$04^h41^m04^s$	62.766	116.5	+79.1	14.6	0.965	0.439	2.28	19.6	150.5	62.763	213.3
			±1.2	±0.6	±0.1	±0.002	±0.015		±0.2	±0.9	±0.001	±0.9
5/24	$05^h15^m59^s$	62.790	71.7	+77.0	9.1	0.943	0.781	1.28	13.2	132.2	62.791	195.0
			±8.8	±4.2	±0.5	±0.025	±0.073		±1.2	±12.5	±0.002	±12.5
5/24	$05^h21^m27^s$	62.793	108.7	+79.1	14.0	0.961	0.491	2.04	19.0	148.3	62.791	211.1
			±9.4	±6.0	±1.1	±0.030	±0.115		±1.8	±10.7	±0.003	±10.7
5/24	$05^h45^m48^s$	62.810	14.4	+79.8	9.8	0.930	0.857	1.17	16.3	121.1	62.809	183.9
			±30.0	±47.9	±2.1	±0.191	±0.290		±7.4	±70.4	±0.054	±70.4
5/24	$06^h41^m14^s$	62.847	125.8	+77.5	16.0	0.968	0.320	3.13	20.6	153.3	62.844	216.1
			±7.6	±2.0	±1.0	±0.026	±0.085		±1.1	±7.5	±0.003	±7.5
5/24	$07^h43^m00^s$	62.888	119.9	+76.9	14.0	0.967	0.441	2.27	18.3	151.2	62.890	214.1
			±1.0	±3.5	±0.3	±0.002	±0.045		±1.1	±0.9	±0.001	±0.9
5/24	$07^h51^m41^s$	62.894	113.2	+77.2	12.8	0.964	0.521	1.92	17.2	148.9	62.894	211.8
			±1.3	±0.9	±0.1	±0.002	±0.017		±0.2	±1.1	±0.001	±1.1
5/24	$08^h11^m43^s$	62.907	109.2	+71.4	12.1	0.958	0.515	1.94	14.9	147.2	62.910	210.1
			±27.9	±51.0	±5.6	±0.162	±0.454		±8.9	±68.9	±12.454	±72.1
5/24	$08^h37^m07^s$	62.924	120.5	+77.9	15.2	0.966	0.383	2.61	19.9	151.6	62.924	214.6
			±0.6	±0.4	±0.1	±0.001	±0.006		±0.2	±0.4	±0.001	±0.4
5/24	$09^h25^m53^s$	62.957	111.5	+73.2	10.5	0.966	0.605	1.65	13.7	147.3	62.962	210.3
			±23.5	±23.2	±1.1	±0.114	±0.248		±5.1	±41.1	±0.175	±41.2
5/24	$09^h37^m39^s$	62.964	89.8	+75.3	6.6	0.963	0.824	1.21	9.5	135.7	62.977	198.6
			±29.7	±54.3	±1.6	±0.173	±0.213		±4.7	±75.1	±5.632	±75.6
5/24	$10^h01^m17^s$	62.980	115.6	+76.9	15.2	0.961	0.381	2.62	19.6	150.4	62.981	213.3
			±10.4	±7.0	±0.1	±0.005	±0.112		±2.3	±2.5	±0.001	±2.5
5/24	$11^h34^m15^s$	63.042	122.8	+78.2	15.3	0.967	0.379	2.64	20.1	152.2	63.043	215.2
			±0.3	±1.6	±0.1	±0.001	±0.022		±0.5	±0.2	±0.001	±0.2
5/24	$22^h27^m23^s$	63.478	117.7	+77.2	8.7	0.975	0.710	1.41	12.4	147.4	63.484	210.9
			±3.5	±1.9	±0.2	±0.006	±0.025		±0.4	±3.4	±0.001	±3.4
209P/LINEAR		65.694	120.6	+73.9	15.8	0.904	0.341	2.932	19.35	150.3	65.691	216.0

Acknowledgements

I thank the SETI Institute board of trustees and CEO David Black for their sponsoring of the aircraft deployment and support of the public outreach effort. Diane Gilbert and Dave Samuels operated cameras that streamed video live to the internet. Esko Lyytinen did the original prediction calculations. CAMS@Benelux station-operators Steve Rau, Klaas Jobse, Martin Breukers, Robert Haas, Felix Bettonvil, Erwin van Ballegoij, Piet Neels and Carl Johannink contributed to this work. Peter Gural developed single-track association algorithms for this work. Jeff Brower, Peter Bus, and Ilkka Yrjola of Global-MS-Net contributed radio forward meteor scatter observations. CAMS is supported by the NASA Planetary Astronomy and NASA Near Earth Object Observation programs.

References

Brown P. (2014). "Camelopardalid meteors". *Central Bureau Electronic Telegrams*, **3886**.

Bus P. (2014). "Radiowaarnemingen van de uitbarsting van de mei camelopardaliden". *eRadiant*. (June 2014 issue, in Dutch).

Gural P. S. and Jenniskens P. (2000). "Leonid storm flux analysis from one Leonid MAC video AL50R". *Earth, Moon and Planets*, **82-83**, 221–247.

International Meteor Organization (2014). "Camelopardalids 2014: visual data quicklook". `http://www.imo.net/live/cameleopardalids2014/` . (last accessed 2014 June 9).

Jenniskens P. (2006). *Meteor Showers and their Parent Comets*. Cambridge University Press, 790 pages.

Jenniskens P. (2008). "Mostly dormant comets and their disintegration into meteoroid sterams: A review". *Earth, Moon and Planets*, **102**, 505–520.

Jenniskens P., Gural P. S., Dynneson L., Grigsby B., Newman K. E., Borden M., Koop M., and Holman D. (2011). "CAMS: Cameras for Allsky Meteor Surveillance to validate minor meteor showers". *Icarus*, **216**, 40–61.

Jenniskens P. and Lyytinen E. (2014). "Possible new meteor shower from comet 209P/LINEAR". *Central Bureau Electronic Telegrams*, **3869**.

Murray I. S., Beech M., Taylor M. J., Jenniskens P., and Hawkes R. L. (2000). "Comparison of 1998 and 1999 Leonid light curve morphology and meteoroid structure". *Earth, Moon and Planets*, **82-83**, 351–367.

Rao J. (2014). "Strong new meteor shower to strike?". *Sky & Telescope*, pages 30–35. (May 2014).

Rudawska R. and Jenniskens P. (2014). "New meteor showers identified in the CAMS and SonotaCo meteoroid orbit surveys". In *Proc. Meteoroids 2013 Conf., Aug. 26-30, 2013*, A.M. University, Poznan, Poland. (in press).

Šegon D., Gural P., Ž. A., Skokić I., Korlević K., Vida D., and Novoselnik F. (2014). "New showers from parent body search across several video meteor databases". *WGN, Journal of the IMO*, **42**, 57–64.

Vaubaillon J. (2003). *Dynamics of meteoroids in the Solar System. Application to the prediction of meteoric showers in general and Leonids in particular*. PhD thesis, I.M.C.C.E., Observatoire de Paris, Paris, France.

Vaubaillon J. (2012). "The next big meteor shower". `http://www.imcce.fr/langues/en/ephemerides/phenomenes/meteor/DATABASE/209_LINEAR/2014/index.php?char=year&body=Earth&year=2014&shower=209_LINEAR` . (last accessed 2014 June 2).

Ye Q. and Wiegert P. A. (2014). "Will comet 209P/LINEAR generate the next meteor storm?". *MNRAS*, **437**, 3283–3287.

Handling Editor: Javor Kac

Exceptionally Persistent Fireball Over the British Isles, 2012 September 21, 21^h55^m–21^h58^m UT

Alastair McBeath[1], *Esko Lyytinen*[2], *Marco Langbroek*[3], *and Robert D. Matson*[4]

Details from trajectory and orbital analyses are presented and discussed concerning an unusually long-lasting, heavily fragmenting, fireball which flew from above northern Germany across the central British Isles between 21^h55^m and 21^h58^m UT on 2012 September 21, ending over the North Atlantic Ocean. The fireball was observed for more than 2^m40^s and its complete visible flight may have lasted five minutes. Its approach angle was shallow, causing it to show a period with a rising trajectory within the atmosphere, before descending again to a probable splashdown point roughly 1500 km off western Ireland about eight minutes after it first became luminous. Meteorites may have fallen on land during the flight, although none were recovered. A comparison between the projected surface tracks determined independently using visual and imaging data was possible, to test the general accuracy of the visual findings. Some discussion of the associated sonics, both electrophonic and acoustic is given too, as well as identifying difficulties found during the analyses, including with some of the imaging data, and the effort involved in sifting through a final 995 individual observations of this meteor.

Received 2014 February 18

1 Introduction

Statistically, particularly slow-moving fireball-class meteors are rare, to the point where apparently bright-meteor-like moving objects seen in the night sky which remain visible for tens of seconds or more are generally assumed to have been non-meteoric. While this is a reasonable proposition in most cases, there is a clear need for caution in making it a general application, after two such genuinely meteoric events were witnessed from large parts of the British Isles during 2012, the first on March 3 (McBeath, 2012), the second the fireball discussed here that took place on September 21.

This September 21 fireball was remarkable for a number of reasons, as like that on March 3, it was witnessed and reported by hundreds of people, and was imaged from numerous widely-separated locations. Unlike the March 3 event however, a few images were of sufficient quality to allow an accurate estimation of the fireball's atmospheric trajectory, beginning within a few days of the event, providing a unique opportunity for a comparison between this instrumentally-established data and what information could be suggested from the comments by the hundreds of visual witnesses. Such a comparison is important, because in recent decades, many well-observed fireballs from the British Isles have been reported exclusively by visual observers. While scarcely conclusive, as based on just one instance, this meteor has meant an estimation of the reliability of the visual-only data could be made on this occasion.

Below, we present findings based on the analysis carried out by the Society for Popular Astronomy's (SPA's) Meteor Section, the early trajectory estimates, and the subsequent more detailed trajectory and orbital information established from the imaging data since the event, with appropriate discussion.

[1]12a Prior's Walk, Morpeth, Northumberland, NE61 2RF, England, UK. Email: spameteors@popastro.com
[2]Kehäkukantie 3 B, 00720 Helsinki, Finland. Email: esko.lyytinen@jippii.fi
[3]Zusterhof 6, 2311 Leiden, The Netherlands. Email: marco@langbroek.org
[4]1 Veneto, Newport Coast, CA 92657, USA. Email: robert.d.matson@leidos.com

IMO bibcode WGN-423-mcbeath-fireball
NASA-ADS bibcode 2014JIMO...42..106M

2 Visual results

As luck had it, the September 21 fireball occurred during the 2012 IMC on La Palma, where the SPA Meteor Director Tony Markham was at the time, out of contact with his home base in the UK. Consequently, it fell to his assistant, AM, to cope with the incoming flood of sightings and reports on the meteor from all parts of the British Isles and beyond. It was clear very quickly that this had been a most unusual meteor, and within days, the number of sightings collected by the SPA had already passed through the previous UK record of 353 reports (on the 2012 March 3 fireball). With some witnesses kindly passing on data from other individuals, or extracts from places where many reports had been filed electronically on the Internet, including social media sites such as Twitter and Facebook, it rapidly became impossible to identify exactly where many sightings had originated. However, several websites were particularly important as having amassed large numbers of reports or links to images and videos, and while some of these duplicated items received from elsewhere, the analysis here included data from the following places (some may need an additional search from the weblink provided to locate the meteor):

- the American Meteor Society's (AMS's) fireball reporting webpage for Event 1379 – access via the AMS homepage[a] (many sightings),
- the Armagh Observatory's fireball reporting webpage[b] (many sightings),
- the "Badastronomy" blog[c],
- the Lunar Meteorite Hunter's website[d] (very many sightings, but often with little detail provided),

[a]http://www.amsmeteors.org
[b]http://arpc65.arm.ac.uk/cgi-bin/fireballs/search.pl
[c]http://blogs.discovermagazine.com/badastronomy/2012/09/21/very-bright-and-spectacular-meteor-seen-over-northern-uk/
[d]http://lunarmeteoritehunters.blogspot.co.uk/

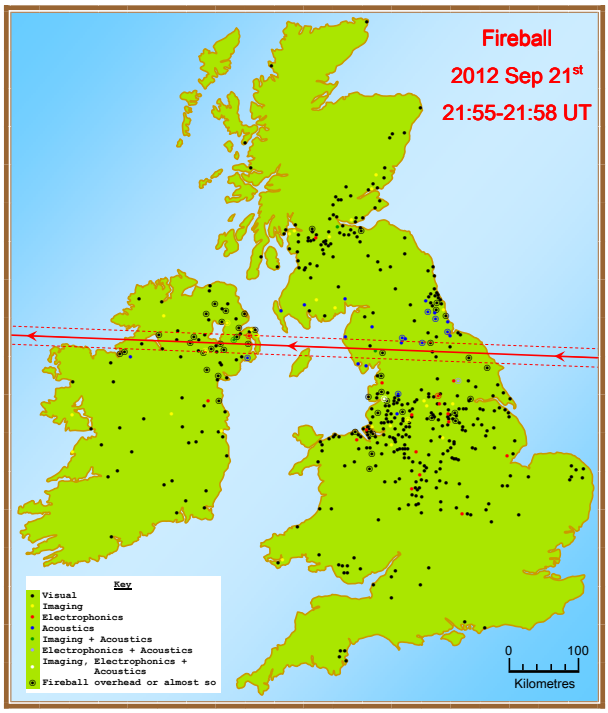

Figure 1 – A sketch map of the British Isles showing details for the September 21, 21^h55^m–21^h58^m UT fireball, with identified places where at least one observer was situated (frequently multiple witnesses were near the same site, particularly for the city centres, up to 23 people in and near central Manchester). On the electronic colour version, various other aspects reported from particular areas are most clearly seen, as indicated by the Key. The arrowed line shows the more probable projected surface track for the fireball as it passed across the British Isles, as derived from the visual reports alone. The north-south likely error limits for this track are indicated by the accompanying dashed lines (note that the arrowed track line might be pivoted approximately within those error limits or be shifted parallel to them).

- the SPA's Observing Forum topic[e], and
- the UK Weather World's Space Weather Forum topic[f].

Excluding duplicates, the final number of separate reports amassed (including videos, images and visual sightings) came to 995. Forty-three included videos or images. Ninety-one reports were from sites which could not be located, either because the witness provided insufficient, or only ambiguous, information, but those which could be identified were scattered across, from west to east, Ireland, Northern Ireland, Scotland, Wales, the Isle of Man, England, the North Sea, the Netherlands, Norway, Germany and Denmark. Figure 1 shows the location of witnesses for the British Isles, where such sites could be established, together with other information reported from those places, and the estimated visual surface track.

The surface track across the British Isles was determined using 66 identifiable locations from where the meteor was claimed as having passed overhead, or almost so, using the methods as previously employed in SPA visual fireball analyses in this journal, so ignoring extreme outliers and attempting to reconcile as many of the remaining sightings as possible, including with the fireball's sky-location as reported from other sites. It was apparent from early in the analysis that no British witnesses had seen the start of the fireball's visible flight. The visible end too seemed to have passed unobserved. In early hopes of determining a possible end area, based on expectations from the preliminary trajectory estimates that included imaging results, data was extracted from those visual reports where numerical end point estimates of altitude $\leq 10°$ had been made. Regrettably, only eleven such reports could be found with identifiable locations, and of those, just three indicated a suitable point off the central-western Irish Atlantic coast, observations made from Leeds in England, Waterloo, Perthshire in Scotland and Birdhill, County Tipperary in Ireland. Given the problems in analysing small-angle altitudes, only the azimuths were used from these three sites to determine a possible end-point. Curiously, the three azimuth lines came within $\sim$ 40 km of crossing one another near 15°.6 W, 53°.6 N, roughly 360 km offshore of Achil Head, Achil Island, County Mayo, Ireland. Figure 3 shows this possible end area, together with the approximate azimuth bearings from the three places, respectively sites 9, 13 and 10.

Many observers provided estimates for how long they were able to see the event. These ranged from 2 to 300 s, the latter almost certainly an exaggeration, with 83% of reported estimates falling between 10 to 60 s, and 76% within 10 to 30 s. Just nine sightings favoured a visibility over sixty seconds, and the average from all 675 reports was 18.9 s. However, the observers involved clearly saw only part of the trail, and while this mean duration may say more for the individual's limited view of the sky, it may also provide a crude ball-park figure relating to the readily-visible interval during which the meteor passed across part of the British Isles.

This aspect was investigated further to try to provide angular velocity figures during the British Isles part of the object's flight. Information was taken from reports where sky-position details were available on the first and last points of the observed visible trail, and where a visible duration estimate had been made too. Unfortunately, only 23 reports, just one from outside the British mainland, included all this information. After computation, these gave a range from 0.1 to 18.7°/s, and a mean of 5.4°/s. Most (74%) fell in the range from 1.5 to 9.5°/s (mean 4.6°/s), with 52% of 2.5 to 8.5°/s (mean 5.1°/s). Such values, however crude, could be compared with imaging-derived data from the flight across northern England especially, as made within about 200 km of the projected surface track, and close to being at right angles to the flight-path.

The fireball most probably began at 21^h55^m UT, drawing on the time-stamp from the earliest image from Norway, site 12 in Figure 3, confirmed following the identification by ML of the NOSS 2-3C satellite (Cospar 1996-029C, SSC 23908) passing across the images simultaneously, and visual details from the Netherlands

[e] http://forum.popastro.com/viewtopic.php?f=1&t=17499
[f] http://www.ukweatherworld.co.uk/forum/index.php?/topic/93871-fireball-report-2258-bst-210912/

(site 3, from where the trail's start was seen). However, the occurrence timing estimates from the observers elsewhere were often at considerable variance with this and one another, with many failing to note even whether British Summer Time (UT +1h) or UT had been used. This was a particular problem with reports from the AMS website where various American time zone abbreviations featured instead, presumably partly through the site's default settings. Where practical, times were assumed as having been meant to be around $21^{\rm h}55^{\rm m}$ UT. Naturally, there were problems in doing so, and the overall range of timings converted to UT from what was claimed ran from $19^{\rm h}15^{\rm m}$ to $00^{\rm h}10^{\rm m}$ UT for what, judging by the descriptions, must have been the same fireball. The mean from all 920 estimates was $21^{\rm h}58^{\rm m}.3$ UT, with 84% falling within ten minutes of $21^{\rm h}58^{\rm m}$, and 72% within five minutes of it. Given the longevity of the event, this may more closely represent the estimated end, or British Isles overflight, time for the fireball, rather than when it started (as people will check the time typically only after seeing such an event).

Although many magnitude estimates were provided by the visual witnesses, the value of these, as commonly with fireballs more generally, was very limited. Comparisons with the Moon or Venus were common, particularly in those from the AMS and Lunar Meteorite Hunter's websites, and a substantial number claimed the event had been of Sun-like or greater brilliance. As there were no reports of blindness, temporary or otherwise, and taking into account the generally normal video and image recordings, such extremes were discounted from further analysis, and conservative brightness levels assumed in cases where leeway was available. For example, given that the waxing crescent Moon had been readily visible in the evening sky over Britain up to a couple of hours before the meteor occurred, any comparison with the Moon was taken to mean the crescent Moon that evening, unless the witness noted otherwise. A further problem was that the fireball had broken up into multiple pieces during its passage over Britain, so it was not always clear exactly what people were giving the brightness of. However, from 381 surviving estimates, a mean magnitude of −9.7 was derived, the range overall from −2 to −15 (albeit all "brighter than full Moon" claims that made no mention of the Sun went into the −15 bin). From the more astronomically-experienced descriptions, a range from magnitude −8 to −11 seemed more plausible, if perhaps only for some of the brighter fragments.

While of extremely little scientific use, the majority of visual reports included notes on the colours seen, and a total of 1374 colour estimates were made (most people described more than one colour as present in some part of the event). These divided up into: red 10%, orange 32%, yellow 17%, green 14%, blue + violet 3%, white 24%.

3 Associated sonics

From the SPA analysis, 31 acoustic and 21 electrophonic reports from 56 claims of sonics associated with the fireball had locations given, allowing them to be plotted on Figure 1.

There was no clear pattern to the acoustic reports of when sounds were reported as heard in relation to the observer's position regarding the probable trajectory. For example, the greatest concentration of such reports was in northeast England (eight reports from the coastal plain between the Rivers Tees to Blyth valleys), yet within 25 km of one another, observers at five sites in County Durham alone noted delays from 30 s to 300 s, with no consistency apparent. However, all but two such reports were from within 60 km of the projected surface track, with only one report from anywhere west of Armagh, Northern Ireland, at Dromahair, County Leitrim in Ireland. That several reports of acoustics were from the northeast coast of England, or very near it, seemed to suggest these sounds may have been associated with the fireball beginning to fragment while still out over the North Sea. A report from a ship heading towards England around 190 km off Cleethorpes, Northeast Lincolnshire (site 14 on Figure 3), noted "flickering light when it was passing over the ship", for instance. If that was the start of the fragmentation, it may have begun around 150–180 km off Whitby, North Yorkshire, assuming the ship to have been heading roughly northwest (no exact details could be established, but the sighting was from the bridge), and that "passing over" meant over the ship's central line/direction of heading.

Intriguingly, all the reports of associated electrophonics from England and Wales were south of the projected surface track, the nearest no closer than 40 km from that line, and the furthest (Daventry, Northamptonshire) nearly 230 km distant. In Scotland, only two such reports were made, both from in or near Glasgow, roughly 150 km to the north, while in Ireland there were just three, two in eastern Northern Ireland (at Newtownards, County Down and Newtownabbey), the third in eastern Ireland at Slane, County Meath. Given the descriptions of what was heard, it seems likely most of these were genuine observations of simultaneous sounds, and in England at least, there was a mild concentration somewhat closer to the meteor's projected ground track (albeit caution is needed here, as this was also in the area of greater population densities around southern Lancashire-Greater Manchester-South and West Yorkshire).

4 Preliminary trajectory analyses

In the immediate aftermath of the event, there was much Internet speculation beyond the meteor community as to what it may have been, including an aircraft on fire, and there was naturally equal interest from meteor observers and analysts regarding the likely trajectory and possible fall-sites for any resultant meteorites. Thanks to the object's very long duration and slow apparent speed, the possibility most in need of rapid investigation was whether it had been a satellite or large piece of space-junk re-entering the atmosphere, rather than a natural meteor, despite the lack of suitable re-entry candidates in the Space-Track TIP-

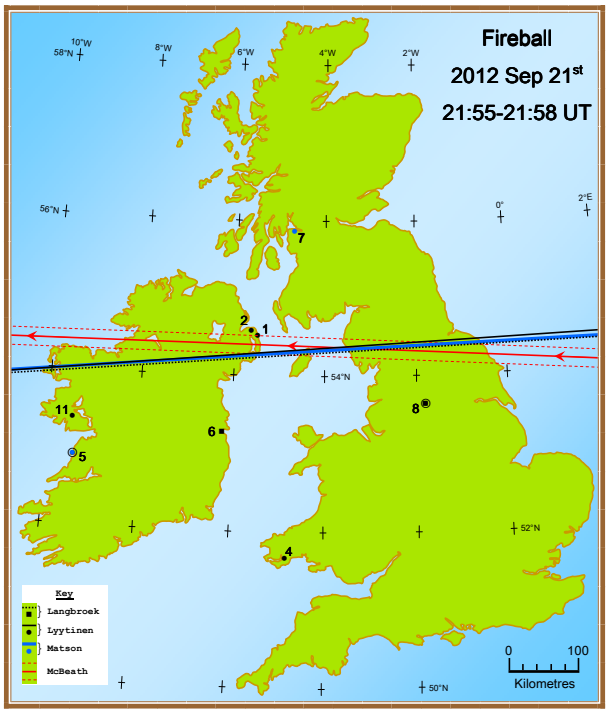

Figure 2 – A similar sketch map to Figure 1, showing the probable projected surface tracks for the 2012 September 21 fireball, as determined by each of this paper's authors using different datasets. The visually-established path, with its likely error margins, has been copied from Figure 1. Sites in the British Isles which contributed to one or more of the analyses by ML, EL and RDM are indicated by numbered symbols (see the caption to Figure 3 for the place-names). Ringed sites contributed to the Lyytinen analysis as well as that indicated by the coloured symbol on the electronic version. The Lyytinen track here is that established by the final analysis from this paper.

messages (which, given the fireball's brilliance, should have been the case if a large enough man-made body had been the source). Drawing on observations from Bussloo in the Netherlands (site 3 on Figure 3), Dublin, Ireland (site 6) and Halifax, England (site 8), ML was able to post preliminary trajectory details online as early as 2012 September 24 (Langbroek, 2012), demonstrating the probable overflight zone for the meteor, and estimating a plausible mean atmospheric velocity of $\sim$ 18 km/s. This provided numerical confirmation that the object had been travelling too swiftly for anything man-made in near-Earth orbit, as well as establishing its east to west path. This latter aspect meant any artificial object in an Earth-centred orbit would have to have been on a retrograde course, which very few Earth-orbiting satellites follow. The line of this projected surface track as it crossed the British Isles, is shown in Figure 2.

A further possibility, because of the object's glancing approach angle, was that part of the original body, perhaps the largest fragment, could have bounced off the atmosphere, but been captured by the Earth's gravity and fallen back to Earth as a second brilliant fireball one orbit later. Intriguingly, just such a fireball had occurred for witnesses in parts of the USA and Canada about 155 minutes after that over northwest Europe. Findings from his initial analysis of this option were published online by RDM on September 25, including the probable projected surface track for the European meteor across the British Isles as established from data at sites 5, 7 and 12, also shown in Figure 2 (the details available in the Meteorite-list archive[g]), while preliminary details from EL's examination followed on September 28 (available in various places online, including the Lunar Meteorite Hunter's website[h]). However, subsequent unpublished analyses by RDM and EL clearly demonstrated the two fireballs had actually been unrelated, from comparisons of their trajectories and velocities.

It would be wrong to imagine these initial investigations were done in isolation from one another, as collaborative discussions and exchanges of data were taking place between all involved from very early on in the process. Indeed it was thanks to these discussions that the decision was taken to analyse the visual reports without reference to the more objective imaging observations, precisely so an estimate of the accuracy of the visual findings could be made. It was also interesting to see how closely the three all-data projected surface tracks matched one another over the British Isles (Figure 2), despite the relatively few datapoints used for the Langbroek and Matson tracks.

5 Final trajectory analysis

Once the initial findings had been published for this fireball, more detailed investigations began. Suspicions that the visible trail's end had passed unobserved were confirmed (images from the most westerly observers in Ireland showed the fireball passing into a heavy cloud bank covering the near-horizon sky), meaning that the later stages of the flight would have to be modelled, rather than calculated from observations. EL was most heavily involved with this final trajectory work, the findings here from that analysis presented for the first time.

The trajectory was derived from calibrated video and imaging data from seven sites (sites 1, 2, 4, 5, 8, 11 and 12 on Figure 3), using the FB_ENTRY Excel program, modified to fit the observations in a non-rotating frame. This was accomplished by altering the longitude values of the observing sites according to the timing. Each observation was given in local azimuth and elevation form, which the program automatically converted to a common frame. The beginning was not imaged, so was determined only from one additional visual observation at Bussloo, Netherlands (site 3). For the track's recorded end, just the main (leading) fragment was considered. Due to the object's low atmospheric entry velocity, the Earth's gravitational effects during the flight needed to be taken into account, as they were significant. The total gravitational curvature was determined as being as large as 9.7°, from the first visual observation to the last recorded point.

[g] http://www.mail-archive.com/meteorite-list@meteoritecentral.com/msg108249.html

[h] http://lunarmeteoritehunters.blogspot.jp/2012/09/breaking-news-uk-earth-hugging-asteroid.html

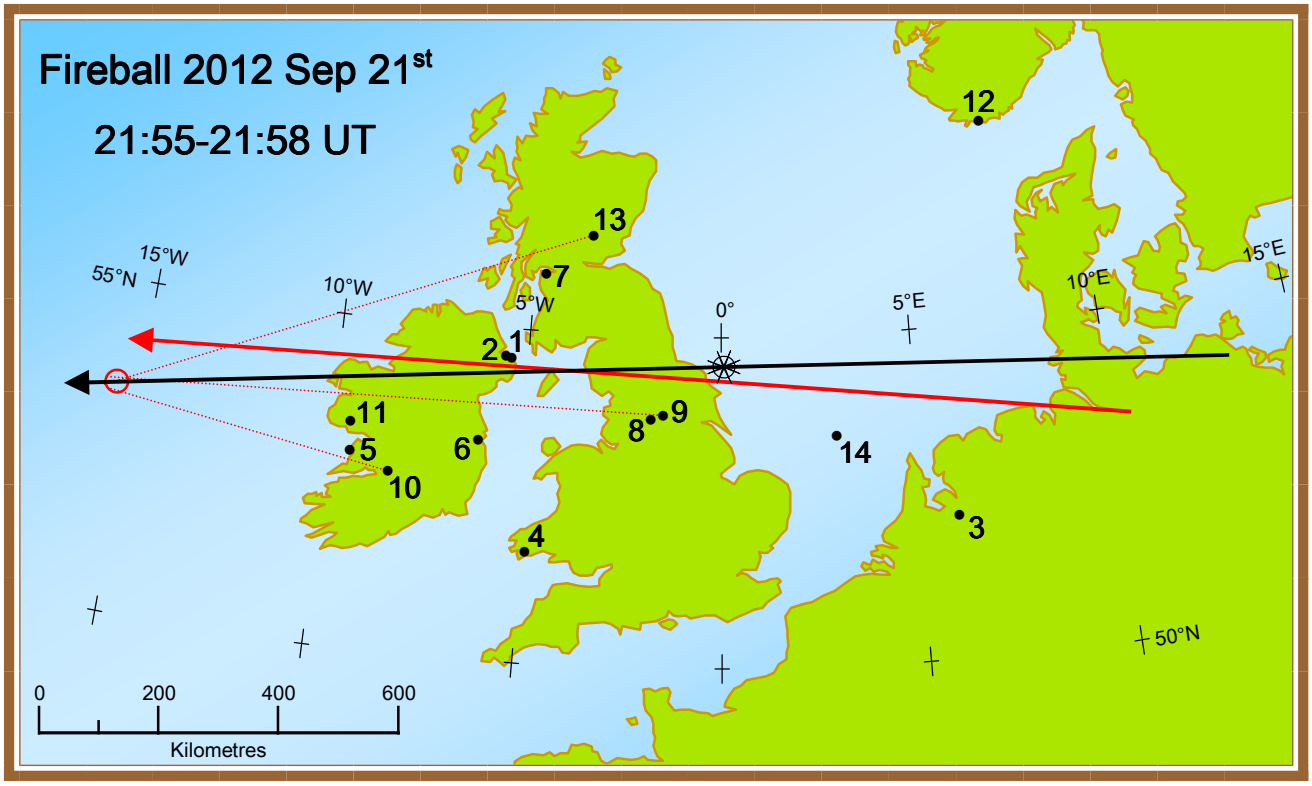

Figure 3 – A sketch-map of part of northwestern Europe, showing selected key locations (numbered dots) for the September 21 fireball. In colour, the red lines and ring-symbol (paler lines in black-and-white) show the visually-estimated projected surface track, and azimuth bearings from sites 9, 10 and 13 to the possible visual end-estimate ring. The black arrowed line shows the final projected surface track for the recorded flight as determined using all sources. The red visual track has been prolonged from Figure 1 to the azimuth bearing for the start as seen from location 3, and to the end longitude shown by the ring. The black starburst-and-circle symbol on the all-sources line indicates the likely earliest fragmentation point during the trail. The site locations were: 1 = Ballyferis Point, Northern Ireland; 2 = Bangor, Northern Ireland; 3 = Bussloo, Netherlands; 4 = Carew Castle, Wales; 5 = Cliffs of Moher, Ireland; 6 = Dublin, Ireland; 7 = Greenock, Scotland; 8 = Halifax, England; 9 = Leeds, England; 10 = Limerick, Ireland; 11 = Maam Cross, Ireland; 12 = Mandal, Norway; 13 = Perth, Scotland; 14 = Unnamed ship at 53°27′.8 N, 2°48′.2 E, North Sea.

Figure 3 shows the observed projected surface track as established in this way (this is effectively identical at this scale to both the preliminary ML and RDM tracks as well), together with that suggested by just the visual reports, here extended beyond the British Isles to match with other parameters.

We wanted to provide a suitable image or two here to help illustrate the fireball's appearance. However, the very long duration of the flight meant no still images, whether taken by standard cameras or as frames extracted and stacked from videos, gave a very clear impression of the object, thus no archetypal "pretty" meteor images of the entire trail, or even parts of it, were available. Instead, we have chosen one of the clearest time-exposure still images showing part of the later observed trail, one which contributed significantly to the final analysis too, Figure 4, with an enlarged segment in Figure 5 to better display some of the finer detail recorded.

This photo demonstrates one of the main aspects of this fireball, that it underwent a series of fragmentation events perhaps lasting for much of its flight across the British Isles, creating a series of glowing trails in the still images. This had both advantages and disadvantages. Positively, it was practical to identify brightenings and fadings along individual fragment trails in comparison with the same events recorded elsewhere with still and video equipment. Equally intriguing was why some fragments showed these light-curve variations, yet others (even at the highest resolution possible) did not. Less helpfully, it meant there was no single, unique path being followed by the fireball during its later observed stages, but instead one which was at least a few kilometres wide. This in turn had implications for what level of accuracy was possible in the analysis overall.

(For example, Figure 4 was taken from a site at approximately 60 km distance to the fireball as it passed closest to being overhead. At that distance, the trigonometry is such that 1° of arc is approximately 1 km, and with an outer angular separation of $\sim 2°$ for the trails nearest the upper left side of the photo, the horizontal distance between them must have been at least 2 km, bearing in mind we do not know the three-dimensional separation of the trails, and the fact this part of the image was not taken at that closest point.)

Exactly where the fragmentation first began, we could not closely define. The ringed starburst symbol near longitude 0° in Figure 3 is located where the last imaged azimuth line from the Mandal, Norway video (site 12) cut the fireball's trajectory, because as far as could be established, there was no definite evidence for fragmentation in those images. It is possible the in-

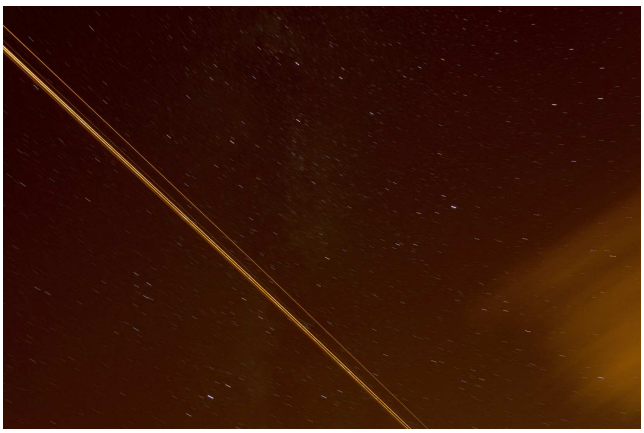

Figure 4 – An image showing the trails created by the passage of the main fragments of the September 21 fireball. The fireball moved top left to bottom right as viewed here, with the trails against the stars of the "Summer Triangle" constellations, Cygnus (centre to top centre), Lyra (centre right) and Aquila (bottom centre left). Taken by Matthew Johnstone near Ballyferis Point, Northern Ireland (site 1 on Figures 2 and 3), using a Nikon D5100 camera with an 18 mm focal-length lens at $f/5.6$, the exposure lasting 148 s. Reproduced by permission.

Figure 5 – An enlargement of the lower part of Figure 4. The star trails of Sagitta lie a little below the meteor trails towards the upper left, while that of the bright star Altair, α Aquilae, is to the lower left.

creasing distance and obliquity to the trail may have masked any small-scale fragmentation, however. Visual reports from eastern England near where the trail first passed over land for Britain suggested the meteor was already fragmenting while still out above the North Sea, something the ship on the North Sea at site 14 seemed to support. Indeed, depending on how that report might be interpreted, it could have suggested some fragmentation was already happening perhaps 100 to 130 km further east. The main fragmentation probably happened, or began, at longitude 1.°6 W, while the meteor was almost passing overhead of Darlington, County Durham, northeast England, as judged by a brightening in the image from site 4. Lesser fragmentation events were recorded by video after this for much of the flight across England at least, probably while over the Irish Sea, and perhaps eastern Northern Ireland too.

Allowing for these factors, and drawing on the best-available data, Figure 6 illustrates details established from the trajectory analysis, showing the fireball's altitude and velocity relative to the surface, as well as its full atmospheric flight. The unobserved part of the flight was determined using a model created by EL, fitted to the observed and derived trajectory characteristics. Table 1 gives the numerical data from which this Figure was created, while Figure 7 provides a three-dimensional graphic representation of the complete trail projected onto the Earth.

As the exact time of the fireball's occurrence could not be precisely determined, only timings relative to the start of the observed flight are given. Salient points during the visible event included the plausible first fragmentation at almost one minute into the flight, the closest approach to the surface at 53.0 km altitude over the extreme eastern part of Northern Ireland around thirty seconds later, and the last observed point just after $2^{\mathrm{m}}40^{\mathrm{s}}$, around 450 km west of the west coast of Achil Island, Ireland. The velocity by that stage had dropped from 12.4 km/s at the start of the flight to 7.7 km/s. Of particular interest is the fact the meteor was observed rising away from the surface towards the end of its visible flight. In general, it is often assumed that meteoric trajectories in the atmosphere are purely descending ones, and for most meteors this is usually correct. In exceptional cases like this object however, with a very shallow approach angle, the meteor may exhibit this type of gentle "bounce" effect, where the degree of curvature of the projectile's incoming path is smaller than that of the Earth's surface. From the modelling, a fresh maximum altitude during this rising phase of 59.6 km was reached at about 185–190 s after the flight began, approximately 600 km offshore of Achil Island. Of course, we cannot know whether the object was still illuminated at this stage, as it was not recorded, but from theoretical considerations, the last luminous part of the trail could have been as late as five minutes after the flight began, as its atmospheric velocity fell below $\sim$ 5 km/s, and if so, that would have been roughly 1300 km west of Achil Head. Assuming it survived intact after it was last recorded, the leading, most massive, fragment may have splashed down into the Atlantic Ocean almost 1500 km from land, a little over eight minutes after the fireball was first seen above northern Germany. Any other surviving larger pieces would have landed in the sea closer to Ireland, but probably still hundreds of kilometres or more from land.

It was not possible to give a very precise estimate for the mass of the original body, but it is probable it was in the range 500–1000 kg, assuming a typical chondritic meteorite density of 3.4 g/cm^3. The leading fragment as the meteor passed above Northern Ireland was estimated similarly as of $\sim$ 100 kg. Converting these values to approximate spherical sizes under the same assumption, yielded an original-body diameter of $\sim$ 0.5–1 m, and a leading fragment diameter of $\sim$ 40 cm.

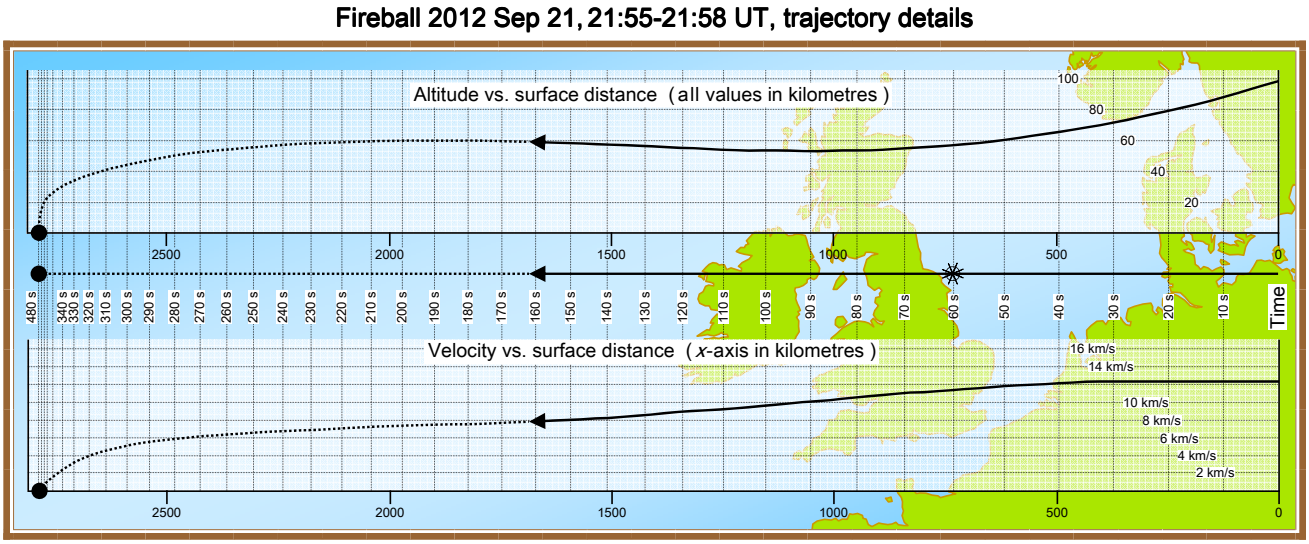

Figure 6 – A diagram based on Figure 3, including the observed surface track for the September 21 fireball (solid arrowed line with the first fragmentation point ringed starburst symbol), here extended to show the full observed plus modelled trajectory (the latter as a dotted line ending in a larger black circle at the probable splashdown area in the North Atlantic Ocean). Vertical time lines during the flight in seconds have been added, with graphs showing the fireball's altitude above mean sea level (upper) and its atmospheric velocity (lower) plotted against time and distance along the trajectory. Note that for clarity, the lines and labels during the rapidly diminishing velocity close to the end of the flight have been deliberately reduced here, and that while both x-axes are drawn to the same scale as the background map, in kilometres, the altitudes on the upper graph have a four times vertical exaggeration.

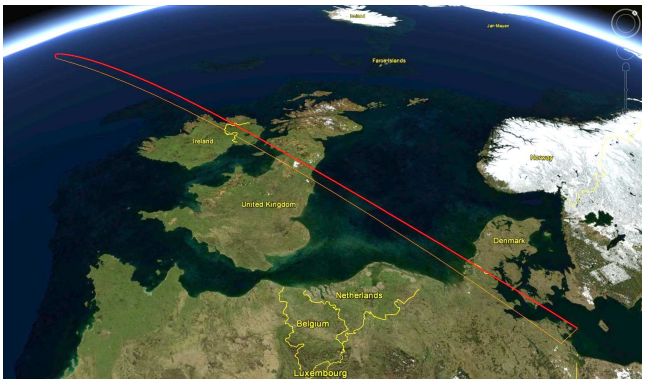

Figure 7 – An illustration showing the full atmospheric flight path (red on the electronic colour version) for the fireball, and its projected surface track (orange – including a linking line to indicate its start elevation), against the spheroidal Earth. Diagram created using Google Earth.

6 Meteorites

One intriguing possibility is that many small fragments, possibly up to several tens of grammes, could have reached the surface along and near the projected surface track of this fireball across the British Isles, especially across Ireland. While it is common to assume any meteorites from a fireball-class meteor will follow along the object's trajectory to drop under gravity at the end of the flight alone, sufficient velocity loss during the flight may cause objects to drop much sooner, notably with low-entry-angle events. This happened recently in the case of the Chelyabinsk meteorite in Russia, which fell on 2013 February 15, where virtually all the objects to land did so at places before the end of the visible flight's surface track (see for example the map at `http://www.niger-meteorite-recon.de/img_inventar/Chelyabinsk_Strewnfield_map_7500.jpg`). EL carried out some dark-flight modelling for the British Isles event, which suggested that chondritic fragments a little less than a kilogramme in mass could have fallen in western Ireland, for instance, assuming no flight-direction change occurred in splitting from the main body. With fragments up to several kilogrammes, such changes of direction by up to circa two degrees could have occurred, and if this deflection was primarily downwards, $\sim$ 5 kg fragments might have made landfall in Ireland. Wind effects at the time, predominantly to the east with a small southerly component, would have been negligible for such larger pieces. For smaller fragments though, over the western part of England say, a drift of up to a kilometre from the projected surface track might have occurred.

One way to have checked for this falling material would have been to use meteorological radar data from around the time the meteor happened, examining the raw data close to the system's noise level to look for potential reflections due to meteoritic dust along the probable flight-line, as it descended to lower stratospheric and tropospheric levels. EL had had some success with this as an experimental technique after the flight of a meteorite-dropping daylight fireball over Finland earlier in 2012. Unfortunately, when we contacted the UK's Meteorological Office to try to obtain data to test similarly following the September 21 meteor, we met with some most unhelpful official obstructions, culminating in the Office requiring us to commit to paying a sum of up to $\sim$ 2500 Pounds Sterling (around 3700 US Dollars-equivalent) before they were prepared to tell us if such information might even exist! Consequently, this aspect of the investigation was not pursued further, although for similar low-velocity events elsewhere, and where an amenable meteorological department might allow such data testing more reasonably, this would be a future option.

Table 1 – Numerical details for the trajectory of the 2012 September 21 fireball, at five-second intervals throughout its observed and modelled flight.

Time (s)	Surface distance (km)	Long. (°)	Lat. (°)	Height above mean sea level (km)	Velocity (km/s)
0	0.0	13.45	53.98	98.5	12.4
5	60.6	12.54	54.07	93.2	12.4
10	121.3	11.62	54.15	88.3	12.3
15	182.0	10.70	54.22	83.6	12.3
20	242.8	9.77	54.28	79.3	12.3
25	303.6	8.84	54.34	75.3	12.3
30	364.5	7.91	54.39	71.6	12.3
35	425.3	6.97	54.44	68.2	12.2
40	485.8	6.04	54.47	65.2	12.0
45	545.5	5.12	54.50	62.5	11.8
50	604.3	4.21	54.52	60.3	11.6
55	662.2	3.32	54.54	58.4	11.4
60	719.2	2.44	54.55	56.8	11.2
65	775.3	1.57	54.55	55.6	11.0
70	830.3	0.72	54.55	54.6	10.8
75	884.3	−0.11	54.54	53.9	10.6
80	937.3	−0.93	54.53	53.4	10.4
85	989.3	−1.73	54.51	53.1	10.2
90	1040.1	−2.52	54.49	53.0	9.9
95	1089.9	−3.29	54.46	53.1	9.7
100	1138.6	−4.04	54.43	53.3	9.5
105	1186.1	−4.77	54.40	53.6	9.3
110	1232.5	−5.48	54.36	54.0	9.0
115	1277.8	−6.17	54.32	54.5	8.9
120	1322.2	−6.85	54.28	55.0	8.7
125	1365.6	−7.51	54.23	55.5	8.5
130	1408.2	−8.16	54.19	56.0	8.4
135	1450.0	−8.79	54.14	56.6	8.2
140	1491.1	−9.42	54.08	57.1	8.1
145	1531.6	−10.03	54.03	57.6	8.0
150	1571.5	−10.63	53.97	58.0	7.9
155	1610.8	−11.22	53.92	58.4	7.8
160	1649.7	−11.80	53.86	58.8	7.7
165	1688.2	−12.38	53.79	59.0	7.7
170	1726.3	−12.95	53.73	59.3	7.6
175	1764.1	−13.51	53.66	59.5	7.6
180	1801.6	−14.06	53.60	59.6	7.5
185	1838.9	−14.62	53.53	59.6	7.5
190	1876.1	−15.16	53.46	59.6	7.5
195	1913.2	−15.71	53.38	59.6	7.4
200	1950.1	−16.24	53.31	59.4	7.4
205	1986.6	−16.77	53.23	59.3	7.3
210	2022.8	−17.30	53.15	59.1	7.2
215	2058.7	−17.82	53.07	58.9	7.1
220	2094.2	−18.33	52.99	58.6	7.1
225	2129.3	−18.83	52.91	58.3	7.0
230	2164.0	−19.33	52.82	57.9	6.9
235	2198.4	−19.82	52.74	57.4	6.8
240	2232.4	−20.30	52.66	56.9	6.8
245	2265.9	−20.78	52.57	56.3	6.7
250	2299.1	−21.25	52.48	55.6	6.6
255	2331.7	−21.71	52.40	54.9	6.5
260	2363.9	−22.16	52.31	54.0	6.4
265	2395.5	−22.61	52.22	53.1	6.3
270	2426.6	−23.04	52.13	52.2	6.2
275	2457.0	−23.47	52.05	51.1	6.0
280	2486.8	−23.88	51.96	50.0	5.9
285	2515.8	−24.29	51.87	48.7	5.7
290	2543.9	−24.68	51.79	47.4	5.6
295	2571.1	−25.05	51.71	46.0	5.4
300	2597.3	−25.42	51.63	44.5	5.2
305	2622.4	−25.76	51.55	42.9	4.9
310	2646.3	−26.09	51.47	41.3	4.7
315	2668.8	−26.40	51.40	39.6	4.4
320	2689.7	−26.69	51.34	37.9	4.0
325	2708.9	−26.95	51.28	36.1	3.7
330	2726.2	−27.19	51.22	34.3	3.3
335	2741.5	−27.40	51.17	32.6	2.9
340	2754.9	−27.58	51.13	30.8	2.5
345	2766.4	−27.74	51.09	29.2	2.2
350	2776.3	−27.88	51.06	27.6	1.9
355	2784.7	−27.97	51.04	26.1	1.6
360	2791.7	−28.05	51.02	24.6	1.3
365	2797.7	−28.11	51.00	23.2	1.1
370	2802.7	−28.16	50.99	21.9	0.9
375	2807.0	−28.20	50.98	20.6	0.8
380	2810.7	−28.23	50.97	19.3	0.7
385	2813.9	−28.26	50.96	18.1	0.6
390	2816.6	−28.28	50.96	17.0	0.5
395	2819.1	−28.29	50.95	15.8	0.5
400	2821.4	−28.30	50.95	14.7	0.5
405	2823.4	−28.31	50.95	13.5	0.4
410	2825.3	−28.32	50.95	12.5	0.4
415	2827.1	−28.33	50.95	11.4	0.4
420	2828.7	−28.33	50.94	10.3	0.3
425	2830.3	−28.34	50.94	9.3	0.3
430	2831.8	−28.34	50.94	8.4	0.3
435	2833.2	−28.34	50.94	7.4	0.3
440	2834.7	−28.34	50.94	6.5	0.3
445	2836.0	−28.34	50.94	5.6	0.3
450	2837.4	−28.34	50.94	4.8	0.2
455	2838.7	−28.34	50.94	4.0	0.2
460	2840.1	−28.34	50.94	3.2	0.2
465	2841.4	−28.34	50.94	2.5	0.2
470	2842.7	−28.34	50.94	1.7	0.2
475	2844.0	−28.34	50.94	1.0	0.2
480	2845.3	−28.34	50.94	0.4	0.1
483	2846.6	−28.34	50.94	0.0	0.1

Despite checking with various places, including limited searching in person in northern England by EL (a happy coincidence possible thanks to a previously-arranged short holiday), no meteorites were recovered after the September 21 fireball. One sighting submitted to Armagh Observatory, made from Newtownabbey, County Antrim, Northern Ireland, did suggest objects had been heard and felt to fall in the vicinity during and soon after the fireball was observed, with 215 fragments recovered for analysis by the witnesses there the following day. Unfortunately, these proved all to be of purely terrestrial origin (personal communication, John Green, 2013 June), and it seemed likely the noises reported were instead electrophonic and acoustic effects due to the meteor.

7 Orbit

After determining the atmospheric trajectory, EL went on to compute an orbit for the original body. Figure 8

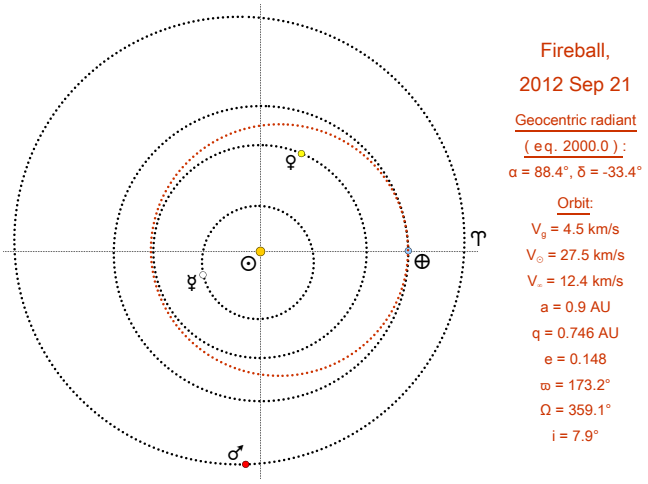

Figure 8 – Orbital data and diagram for the September 21 fireball, shown projected against the paths of the terrestrial planets in the inner Solar System (fireball's path and data in red on the electronic version).

illustrates and numerically defines this orbit, including the geocentric radiant for the fireball. The apparent radiant as derived from the observations was at $\alpha = 59\overset{\circ}{.}2$, $\delta = +2\overset{\circ}{.}9$, around 3° southwest of the fourth-magnitude star ν Tauri in southwestern Taurus. Although no uncertainties are shown, there was quite a degree of these in many of the parameters away from near-Earth space, which could often not be closely defined, so the orbit should be treated as approximate only. For example, the error for the atmospheric entry velocity, V_∞, was estimated as up to ±0.5 km/s. The orbit was of Aten-type, although whether the body had been diverted onto such an orbit through a past close encounter with a terrestrial planet, as is usually supposed for the Aten asteroids, or whether it may even have originated within the Earth-Moon system, could not be definitively-established from this information.

8 Comparison of the visual and imaging trajectories

The reason behind examining the visual reports in isolation from the other data, was to allow a comparison with the more precise parameters for the fireball established by the imaging results, and so give an idea of the relative accuracy of just the visual findings, to help better calibrate those fireball investigations where no useful images or videos were available. From Figure 2, the projected visual surface track across the British Isles was tolerably close to the instrumental ones, enough to give a degree of confidence that previous visual-only fireball analyses of similar kind have probably enjoyed a similar relationship, so likely falling within ∼ 40–50 km of their "true" tracks for the more densely-populated areas at least. However, the visual track is clearly at an angle to the imaging one, pivoted about a point in southwest Cumbria, England, not far from the town of Ambleside. This has almost certainly resulted from the relative population densities – and hence witness numbers of those claiming the meteor passed overhead or almost so – in northern England, statistically "pulling" the English part of the trajectory southwards. A similar effect forcing the trajectory northwards, seems likely to have happened from reports in eastern Northern Ireland, in combination creating the observed effect. Although some attempt to correct for the relative population concentrations had been made, it was obviously insufficient in this case.

When expanded outwards to try to give the complete observed surface track in Figure 3, the problem of this angled line naturally became greater. While the general trend of the track can be treated as correct, the start and last visible points are well away from their most probable ones established instrumentally. That in turn has implications for attempting to estimate the atmospheric trajectory from just the visual data. One curiosity is the relative precision of the "last observed" area given by the visual azimuth estimates at sites 9, 10 and 13. This may simply have been coincidental, but it is rather pleasing nonetheless!

Angular velocities were computed for places at 100 and 200 km distance from the projected surface track in northern England, as established from the final trajectory analysis, giving values of 4.8 and 2.6°/s respectively. The mean visually-established angular velocities of ∼ 4.6 to 5.4°/s spanned the 100 km calculated value quite closely at least. In more detail though, the mean visual values remained similar for observers almost exactly 100 and 200 km from the surface track, at ∼ 5.2°/s each, albeit the number of reports involved was reduced to just three and eight of the twenty-three respectively, so the significance of this finding is doubtful.

Ordinarily, all the available data would have been used in determining the projected surface path and trajectory for such a fireball, and in this case, these would definitely have caused the visual surface track to have been adjusted to coincide with the imaging one, thanks to the quality of the imaging data available. It is interesting that despite all the technology employed, the start point was determined purely thanks to one reliable visual witness in the Netherlands, a clear indication that all data on a fireball may be potentially valuable.

9 Problems with the analyses

While imaging meteor data are rightly lauded as providing much more objective and more readily analyzable results than visual reports, they are far from infallible, particularly when a wide variety of imaging systems has been used to try to capture part of the flight of an object like the September 21 fireball. Of the 43 photographic and video reports, just eight were of sufficient quality to feature in one or other of the trajectory analyses presented in this paper. Those unused were generally because the images were of too poor quality, or showed too few identifying features (stars, stable landmarks), or because the observers' locations could not be sufficiently well established. Even with the used images, not all were ideal. For example, the key automated video time-lapse images from Norway, essential for studying the early flight which passed otherwise unrecorded, showed a degree of variable zooming had occurred during the

imaging, which in turn created considerable problems in trying to accurately measure the meteor's sky position. Fortunately, these were largely overcome during the final analysis, but could not have been anticipated in advance. This is an element which those operating similar automated cameras for meteor work may need to be aware of, where the camera's focus may not be so firmly fixed as expected.

Probably the single greatest difficulty for analysts of this fireball was the sheer volume of observations collected. Well over a thousand reports had to be carefully sifted to exclude duplicates and to extract all the important details from each. The usual follow-up queries were greatly hampered by many sightings having been reported online in formats where no contact address was available, and it proved impossible to clarify many missing or incorrect aspects simply because of the time required to do so. This raises the question as to whether it is worthwhile to try to analyse such a vast number of largely visual, or low-quality imaging, reports. There are definite elements that human witnesses are able to contribute better than using any other method currently available, most particularly the detection of possibly associated sonics, whether electrophonic or acoustic, although these did not provide much readily analyzable data here. Where no, or too few, images are available, there is no other choice than to use visual information if any analysis attempt is to be made, of course. Some items though, such as identifying the geographic spread of a fireball's witnesses, could be likely accomplished better using an automated system, as is already the case with, for instance, the AMS's online fireball reports. Overall, it is probably necessary to deal with future events on a case-by-case basis, but given that the vast majority of casual fireball sightings submitted to online forums in this instance contained very few useful details, the most important aspect is to be able to identify quickly which ones do contain valuable comments, and which others then can be simply ignored, or set aside for possible later investigation (of the sonics, perhaps).

10 Conclusion

An unusual, long-lived fireball of this nature causes us to reassess what "expected facts" we may find with fireball observations more generally. It was observed for more than two-and-a-half minutes, and its entire visible flight may have lasted five minutes, during which time it travelled more than 2500 km. No witnesses saw it start and end; indeed, no witnesses seemed to have observed its end at all. It showed a rising trajectory for part of its flight, not the simple purely descending one we might have intuitively predicted. Meteorites may have begun falling to the surface soon after the object began to fragment, perhaps some 700–800 km into its atmospheric path, again not something that would be typically thought likely. While rare, as meteor analysts we all need to be aware of what surprises such fireballs can sometimes spring!

11 Acknowledgements

We wish to thank all the lucky witnesses of this fireball for their contributed reports, most especially those who were able to provide further detailed information beyond their initial sightings, and those administrators of the various online fireball reporting systems who helped enable us to do so. We also wish to acknowledge considerable assistance from Dirk Ross in locating online images and videos suitable to help with the analysis, in the period soon after the fireball took place.

References

Langbroek M. (2012). "More on the 21 September 2012 fireball: why it definitely was a meteor". `http://sattrackcam.blogspot.nl/2012/09/more-on-21-september-2012-fireball-why.html` .

McBeath A. (2012). "SPA Meteor Section Results: Unusual Long-Lived Fireball, 2012 March 3, 21h41m-21h42m UT". *WGN, Journal of the IMO*, **40:3**, 91–93.

Handling Editor: Javor Kac
This paper has been typeset from a LaTeX file prepared by the authors.

Preliminary results

Results of the IMO Video Meteor Network — February 2014

Sirko Molau[1], *Javor Kac*[2], *Stefano Crivello*[3], *Enrico Stomeo*[4], *Geert Barentsen*[5], *Rui Goncalves*[6], *and Antal Igaz*[7]

The 2014 February results of the IMO Video Meteor Network are summarized. The procedure for population index calculation was scrutinized to explain deviations from the population index obtained from visual observations. No errors in the calculation procedure were found.

Received 2014 May 11

1 Introduction

Eighty cameras contributed to the IMO Network in February. As in the previous month, the weather was sympathetic to the more northern observers in Europe (The Netherlands, Germany, Poland) and presented them with an unusually high number of clear nights. Observers in more southern countries like Spain, Italy, Slovenia or Hungary had to live with much fewer clear nights. Fourteen cameras managed to obtain observations in twenty or more nights, again more than half of them in Germany. Overall we recorded over 14 000 meteors in those 28 February nights during almost 7 000 hours of effective observing time (Table 1 and Figure 1). That is clearly more than in the previous year (Molau et al., 2013) and only 10% below the total of the record-breaking year 2012 (Molau et al., 2012).

Jörg Strunk started to operate his fifth camera named Mincam6, another Mintron camera with 6 mm $f/0.8$ Computar lens. The fight for the pole position in the country statistics of the IMO Network remains thrilling, as the Hungarian observers have plans for further camera stations.

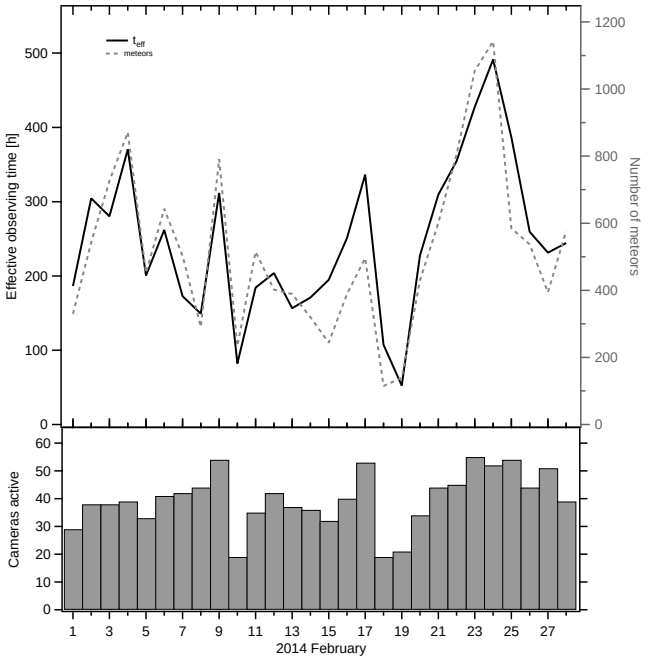

Figure 1 – Monthly summary for the effective observing time (solid black line), number of meteors (dashed gray line) and number of cameras active (bars) in 2014 February.

2 Population index calculation revisited

Since the meteor activity in February is not surprising, we will further analyse the new procedure for population index calculation from video observations at this point. So far, the analyses resulted in smaller r-values than expected, which is why the procedure was checked for possible error sources:

- Determination of meteor brightness: it is a known fact that the meteor brightness values calculated by MetRec often show large errors. This has no impact on the new procedure, however, since the only thing that counts is the number of meteors recorded by a camera at a given limiting magnitude.

- Determination of limiting magnitude: currently a number of video frames are averaged to reduce the noise. A high-pass filter is applied to the mean image to extract point sources. Their position is matched against a star catalog, and the limiting magnitude is deduced from the number of identified stars. If some parameters are adjusted differently (e.g. the threshold to extract point sources), the calculated limiting magnitude will change systematically. That has an impact on the flux density, but not on the population index, since that is calculated from the ratio of cumulative meteor counts in successive magnitude classes. This ratio will remain the same if the limiting magnitude is changed by a constant value.

[1]Abenstalstr. 13b, 84072 Seysdorf, Germany.
Email: sirko@molau.de
[2]Na Ajdov hrib 24, 2310 Slovenska Bistrica, Slovenia.
Email: javor.kac@orion-drustvo.si
[3]Via Bobbio 9a/18, 16137 Genova, Italy.
Email: stefano.crivello@libero.it
[4]via Umbria 21/d, 30037 Scorze (VE), Italy.
Email: stom@iol.it
[5]University of Hertfordshire, Hatfield AL10 9AB, United Kingdom. Email: geert@barentsen.be
[6]Urbanizacao da Boavista, Lote 46, Linhaceira, 2305-114 Asseiceira, Tomar, Portugal. Email: rui.goncalves@ipt.pt
[7]Húr u. 9/D, H-1223 Budapest, Hungary.
Email: antaligaz@yahoo.com

IMO bibcode WGN-423-molau-vidfeb
NASA-ADS bibcode 2014JIMO...42..116M

- Detection probability of meteors: currently an idealized step function is used, according to which MetRec will detect 100% of all meteor up to the limiting magnitude, but no meteor beyond. In reality, the detection rate will decline slowly as the limiting magnitude is approached. The effect will be less dramatic than for visual observers, but it will not be a step function. This effect also has only an impact on the flux density, but not on the population index. The reason is that we do not analyse intervals of the same meteor brightness, but of the same limiting meteor magnitude of the camera. So a systematically lower detection probability has the same effect on all intervals.

- Zenith exponent: beside the population index the zenith exponent has a significant impact on the number of observed meteors – in particular for low radiant altitudes and slow meteor showers. A quick test has shown, though, that the zenith exponent impacts primarily the flux density, but not the determined population index.

- Programming errors: to check that the procedure is working properly, a real observation was taken (observing time, limiting magnitudes, effective collection areas of cameras) and the observed meteors were replaced by simulated meteors. During the simulation, each meteor was characterized by three random numbers:

  – One represented the meteor brightness, whereby the overall distribution was chosen such that it matched a given population index.

  – One simulated the direction in the sky, whereby cameras with twice as large field of view had a chance twice as high that the meteor appeared "inside" the field of view.

  – One represented the number of meteors per minute, based on a Poisson distribution.

  A meteor was counted as "observed" if it was inside the field of view and brighter than the limiting meteor magnitude of the camera.

  The simulation was carried out for different r-values and it was checked if the procedure obtained the predefined population indices. The result was encouraging – there were only minor systematic deviations such that the r-value was overestimated by 0.1 to 0.2. The root cause of this deviation is currently not clear, but it seems that the determined r-values are rather a little too big than too small.

A discussion at the Arbeitskreis Meteore (AKM) spring seminar revealed, that deviations between the visual r-values and those obtained from video observations would be possible, since both are based on different boundary conditions:

- Video observations are using the absolute meteor magnitude (i.e. normalized to 100 km altitude), visual observation the apparent magnitude.

- The observing direction (altitude, radiant distance) is accounted for in case of video observations, but not for visual observations.

- The loss in limiting magnitude from the meteor motion (fast meteors distribute their photons over more pixels) is accounted for in case video observations, but not for visual observations.

Thus, the recently obtained population indices match our expectations.

References

Molau S., Kac J., Berko E., Crivello S., Stomeo E., Igaz A., and Barentsen G. (2012). "Results of the IMO Video Meteor Network - February 2012". *WGN, Journal of the IMO*, **40:3**, 101–107.

Molau S., Kac J., Berko E., Crivello S., Stomeo E., Igaz A., Barentsen G., and Goncalves R. (2013). "Results of the IMO Video Meteor Network - February 2013". *WGN, Journal of the IMO*, **41:3**, 92–95.

Handling Editor: Javor Kac

Table 1 – Observers contributing to 2014 February data of the IMO Video Meteor Network. Eff.CA designates the effective collection area.

Code	Name	Place	Camera	FOV [°²]	Stellar LM [mag]	Eff.CA [km²]	Nights	Time [h]	Meteors
ARLRA	Arlt	Ludwigsfelde/DE	Ludwig2 (0.8/8)	1534	5.8	2467	22	160.1	406
BERER	Berkó	Ludányhalászi/HU	Hulud3 (0.95/4)	4357	3.8	876	4	41.8	40
BOMMA	Bombardini	Faenza/IT	Mario (1.2/4.0)	5794	3.3	739	9	37.5	114
BREMA	Breukers	Hengelo/NL	Mbb3 (0.75/6)	2399	4.2	699	19	142.8	153
			Mbb4 (0.8/8)	1470	5.1	1208	16	117.1	107
BRIBE	Klemt	Herne/DE	Hermine (0.8/6)	2374	4.2	678	20	135.9	219
		Bergisch Gladbach/DE	Klemoi (0.8/6)	2286	4.6	1080	19	112.9	163
CASFL	Castellani	Monte Baldo/IT	Bmh1 (0.8/6)	2350	5.0	1611	11	30.3	136
			Bmh2 (1.5/4.5)*	4243	3.0	371	13	82.7	136
CRIST	Crivello	Valbrevenna/IT	Bilbo (0.8/3.8)	5458	4.2	1772	16	76.7	163
			C3P8 (0.8/3.8)	5455	4.2	1586	13	86.9	122
			Stg38 (0.8/3.8)	5614	4.4	2007	14	55.0	156
DONJE	Donani	Faenza/IT	Jenni (1.2/4)	5886	3.9	1222	16	94.5	263
ELTMA	Eltri	Venezia/IT	Met38 (0.8/3.8)	5631	4.3	2151	9	60.0	103
GANKA	Gansel	Dingden/DE	Daro01 (1.4/3.6)	7141	3.1	652	18	113.4	122
GONRU	Goncalves	Tomar/PT	Templar1 (0.8/6)	2179	5.3	1842	10	66.2	92
			Templar2 (0.8/6)	2080	5.0	1508	15	89.0	133
			Templar3 (0.8/8)	1438	4.3	571	13	64.3	52
			Templar4 (0.8/3.8)	4475	3.0	442	14	68.0	109
			Templar5 (0.75/6)	2312	5.0	2259	20	81.8	113
GOVMI	Govedič	Središče ob Dravi/SI	Orion2 (0.8/8)	1447	5.5	1841	13	70.1	117
			Orion3 (0.95/5)	2665	4.9	2069	8	36.5	45
			Orion4 (0.95/5)	2662	4.3	1043	7	6.0	37
HERCA	Hergenrother	Tucson/US	Salsa3 (1.2/4)*	2198	4.6	894	27	249.8	357
IGAAN	Igaz	Baja/HU	Hubaj (0.8/3.8)	5552	2.8	403	6	18.5	39
		Debrecen/HU	Hudeb (0.8/3.8)	5522	3.2	620	11	71.9	86
		Hódmezővásárhely/HU	Huhod (0.8/3.8)	5502	3.4	764	14	83.7	107
		Budapest/HU	Hupol (1.2/4)	3790	3.3	475	8	52.8	19
JONKA	Jonas	Budapest/HU	Husor (0.95/4)	2286	3.9	445	14	74.1	107
KACJA	Kac	Ljubljana/SI	Orion1 (0.8/8)	1402	3.8	331	5	19.5	7
		Kamnik/SI	Cvetka (0.8/3.8)*	4914	4.3	1842	5	16.7	28
			Rezika (0.8/6)	2270	4.4	840	4	18.1	38
			Stefka (0.8/3.8)	5471	2.8	379	5	14.7	23
		Kostanjevec/SI	Metka (0.8/12)*	715	6.4	640	1	9.3	15
KERST	Kerr	Glenlee/AU	Gocam1 (0.8/3.8)	5189	4.6	2550	12	41.8	188
KISSZ	Kiss	Sülysáp/HU	Husul (0.95/5)*	4295	3.0	355	11	63.9	26
KOSDE	Koschny	Izana Obs./ES	Icc7 (0.85/25)*	714	5.9	1464	24	186.3	991
		La Palma/ES	Icc9 (0.85/25)*	683	6.7	2951	23	183.6	1403
		Noordwijkerhout/NL	Lic4 (1.4/50)*	2027	6.0	4509	21	143.4	237
LOJTO	Łojek	Grabniak/PL	Pav57 (1.0/5)	1631	3.5	269	7	35.5	34

Table 1 – Observers contributing to 2014 February data of the IMO Video Meteor Network – continued from previous page.

Code	Name	Place	Camera	FOV [°²]	Stellar LM [mag]	Eff.CA [km²]	Nights	Time [h]	Meteors
MACMA	Maciejewski	Chełm/PL	Pav35 (0.8/3.8)	5495	4.0	1584	19	111.9	206
			Pav36 (0.8/3.8)*	5668	4.0	1573	20	139.6	222
			Pav43 (0.75/4.5)*	3132	3.1	319	16	92.1	52
			Pav60 (0.75/4.5)	2250	3.1	281	18	104.3	130
MARGR	Maravelias	Lofoupoli-Crete/GR	Loomecon (0.8/12)	738	6.3	2698	7	35.5	60
MASMI	Maslov	Novosibirsk/RU	Nowatec (0.8/3.8)	5574	3.6	773	15	90.1	163
MOLSI	Molau	Seysdorf/DE	Avis2 (1.4/50)*	1230	6.9	6152	20	140.9	729
			Mincam1 (0.8/8)	1477	4.9	1084	22	150.2	218
		Ketzür/DE	Remo1 (0.8/8)	1467	6.5	5491	24	142.6	643
			Remo2 (0.8/8)	1478	6.4	4778	23	164.5	496
			Remo3 (0.8/8)	1420	5.6	1967	16	127.2	88
			Remo4 (0.8/8)	1478	6.5	5358	24	171.1	611
MORJO	Morvai	Fülöpszállás/HU	Huful (1.4/5)	2522	3.5	532	17	111.3	110
MOSFA	Moschner	Rovereto/IT	Rover (1.4/4.5)	3896	4.2	1292	13	61.5	124
OTTMI	Otte	Pearl City/US	Orie1 (1.4/5.7)	3837	3.8	460	18	161.2	302
PERZS	Perkó	Becsehely/HU	Hubec (0.8/3.8)*	5498	2.9	460	13	77.8	140
PUCRC	Pucer	Nova vas nad Dragonjo/SI	Mobcam1 (0.75/6)	2398	5.3	2976	9	37.2	53
QUIVI	Quinta	Azeitao/PT	Azeit1 (1.2/6)	2354	—	—	8	69.8	37
ROTEC	Rothenberg	Berlin/DE	Armefa (0.8/6)	2366	4.5	911	17	127.7	123
SARAN	Saraiva	Carnaxide/PT	Ro1 (0.75/6)	2362	3.7	381	15	87.5	82
			Ro2 (0.75/6)	2381	3.8	459	16	86.1	99
			Ro3 (0.8/12)	710	5.2	619	13	69.5	76
			Sofia (0.8/12)	738	5.3	907	14	89.5	86
SCALE	Scarpa	Alberoni/IT	Leo (1.2/4.5)*	4152	4.5	2052	5	15.0	23
SCHHA	Schremmer	Niederkrüchten/DE	Doraemon (0.8/3.8)	4900	3.0	409	24	152.7	321
SLAST	Slavec	Ljubljana/SI	Kayak1 (1.8/28)	563	6.2	1294	4	21.2	36
STOEN	Stomeo	Scorze/IT	Min38 (0.8/3.8)	5566	4.8	3270	16	74.2	296
			Noa38 (0.8/3.8)	5609	4.2	1911	14	71.3	199
			Sco38 (0.8/3.8)	5598	4.8	3306	16	83.0	313
STRJO	Strunk	Herford/DE	Mincam2 (0.8/6)	2354	5.4	2751	18	128.1	312
			Mincam3 (0.8/6)	2338	5.5	3590	18	126.5	236
			Mincam4 (1.0/2.6)	9791	2.7	552	11	94.0	154
			Mincam5 (0.8/6)	2349	5.0	1896	17	121.1	231
			Mincam6 (0.8/6)	2395	5.1	2178	19	123.5	233
TEPIS	Tepliczky	Agostyán/HU	Huago (0.75/4.5)	2427	4.4	1036	17	135.2	175
		Budapest/HU	Humob (0.8/6)	2388	4.8	1607	19	139.3	221
TRIMI	Triglav	Velenje/SI	Sraka (0.8/6)*	2222	4.0	546	10	28.3	69
YRJIL	Yrjölä	Kuusankoski/FI	Finexcam (0.8/6)	2337	5.5	3574	1	10.2	13
ZELZO	Zelko	Budapest/HU	Huvcse03 (1.0/4.5)	2224	4.4	933	3	10.6	15
			Huvcse04 (1.0/4.5)	1484	4.4	573	4	13.2	16
* active field of view smaller than video frame						Overall	28	6 909.6	14 519

Results of the IMO Video Meteor Network — March 2014

Sirko Molau[1], *Javor Kac*[2], *Stefano Crivello*[3], *Enrico Stomeo*[4], *Geert Barentsen*[5], *Rui Goncalves*[6], *and Antal Igaz*[7]

The best March result for the IMO Video Meteor Network was obtained this year, with more than 20 000 meteors recorded by 80 cameras in almost 12 000 hours of observing time. A Watec 910HX-RC camera is introduced and tested on stars, but not yet put to a real-life test on meteors.

Received 2014 June 17

1 Introduction

March 2014 was another record-breaking month. The lucky streak continued for the observers in northern Europe, who where already enjoying unusually good weather in the previous months. At the same time the observers in southern and eastern Europe finally experienced better observing conditions after a long lean period. In total, 58 out of 80 cameras, i.e. more than 70%, managed to observe during twenty or more nights. During three nights (March 12/13, 13/14 and 28/29) an amazing 72 cameras were active at the same time, which is another splendid result.

In the history of the IMO Network there are just two months (October 2011 and August 2012) where we collected more than 10 000 hours of effective observing time. Thanks to the combination of perfect weather and relatively long nights in March, we collected almost 12 000 hours this month (Table 1 and Figure 1), which set new standards. On the other hand, the typical "spring minimum" of meteor activity was particularly strong this year — 1.7 meteors per hour was the lowest average yield since 2005. Hence, when it comes to the sheer meteor number, the month could obviously not compete with August or October, but never before were more than 20 000 meteors recorded in March. Figures 4 and 5 show some interesting meteors in this month.

After the two image-intensified cameras Akm1 and Akm2 of the "Arbeitskreis Meteore" broke down recently, the German meteor observer society purchased another camera. This time we chose a Mintron 12V6-EX without an image intensifier, and a Panasonic 6 mm $f/0.75$ C-mount lens. This camera is operated by 18 year old Kevin Förster of Thuringia, who became the youngest video observer in Germany and maybe even of the whole IMO Network. We wish him that his interest in astronomy will last for a long time.

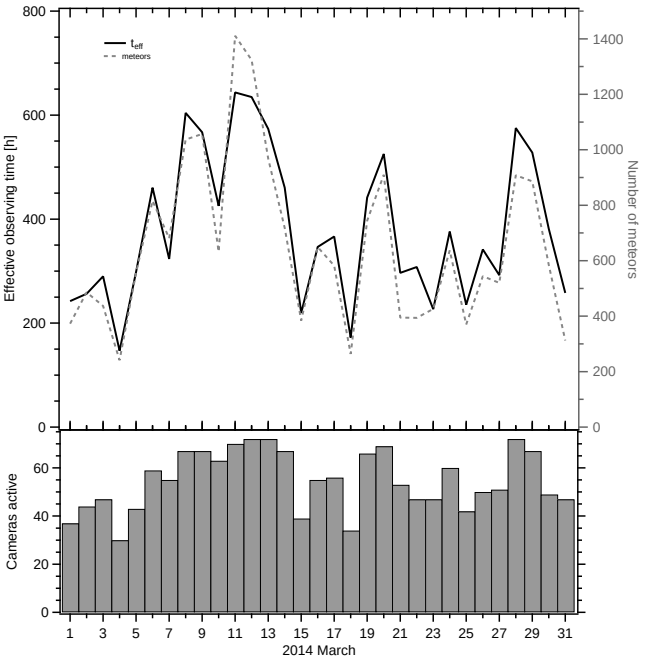

Figure 1 – Monthly summary for the effective observing time (solid black line), number of meteors (dashed gray line) and number of cameras active (bars) in 2014 March.

2 Alternative camera testing

Since March lacks interesting meteor showers, we will have a closer look at video equipment this time. About a month ago, Sirko Molau met "veteran" lunar occultation observer Eberhard Bredner at a meeting of the German "Vereinigung der Sternfreunde" society, and by chance they came to a discussion about video cameras. The requirement of occultation watchers are partly comparable to ours, because occultation events are often faint and of short duration just like meteors. SM was surprised to learn that the occultists neither prefer the Mintron 12V6-EX nor the Watec 902H2 Ultimate, but rather another camera that SM had never heard of before: the Watec 910HX-RC (Figure 2).

This camera is almost twice as expensive and also offers frame integration, which the Watec 902 does not have — but that is something that is hardly a benefit in meteor observation with the fast moving targets. Still, we decided to investigate further.

Thanks to the mediation of Bernd Gährken, Nimax GmbH (`astroshop.de`) was kind enough to provide SM with two cameras for testing, so that he could compare the Mintron and the Watec side-by-side under real observing conditions. A 6 mm $f/0.75$ Panasonic lens was used which is frequently used among meteor observers.

[1]Abenstalstr. 13b, 84072 Seysdorf, Germany.
Email: `sirko@molau.de`
[2]Na Ajdov hrib 24, 2310 Slovenska Bistrica, Slovenia.
Email: `javor.kac@orion-drustvo.si`
[3]Via Bobbio 9a/18, 16137 Genova, Italy.
Email: `stefano.crivello@libero.it`
[4]via Umbria 21/d, 30037 Scorze (VE), Italy.
Email: `stom@iol.it`
[5]University of Hertfordshire, Hatfield AL10 9AB, United Kingdom. Email: `geert@barentsen.be`
[6]Urbanizacao da Boavista, Lote 46, Linhaceira, 2305-114 Asseiceira, Tomar, Portugal. Email: `rui.goncalves@ipt.pt`
[7]Húr u. 9/D, H-1223 Budapest, Hungary.
Email: `antaligaz@yahoo.com`

IMO bibcode WGN-423-molau-vidmar
NASA-ADS bibcode 2014JIMO...42..120M

Figure 2 – Two tested cameras: Watec 910HX-RC (left) and Mintron 12V6-EX (right).

Figure 3 – Reference image of the Watec 910HX-RC (left) and the Mintron 12V6-EX cameras (right), averaged over 64 video frames.

Both cameras were set to 2× sense up (a camera function which sums the individual video frames, resulting in a 2 frame total integration time 1/25 s) which is the default setting for MetRec. The gain was turned to maximum (Watec: AGC high; Mintron: maximum manual gain) and the gamma value was set to 0.45 to enhance dark objects.

Skies in June are not perfectly dark, but visually a limiting magnitude of almost +6 could be obtained in the zenith. The first look at the monitor quickly revealed significant differences. The video image of the Watec was much more noisy — in particular the vertical structures are disturbing — but many more stars could be spotted. In comparison, the Mintron had almost a noise-free image, even at the highest gain level, but fewer stars were visible (Figure 3). The night sky was recorded with both cameras for about 15 minutes for later analysis. The two meteor cameras Avis2 and Mincam1, which were active in parallel, detected only a minor change in limiting magnitude of about 0.1 magnitude, so that the observing conditions must have been almost constant.

During the measurement of the reference image, 76 stars of the Watec image could be used, but only 46 stars of the Mintron. Now the question was: Would the noise of the Watec camera increase in the same manner as the object brightness and thereby kill the gain in limiting magnitude?

The faintest visible star in the field of view is not a good indicator for the limiting magnitude, since it heavily depends on individual factors like the spectral class of a star. For this reason, MetRec uses, similar to visual meteor observers, a more robust procedure to determine the limiting magnitude. At first, all stars in the (slightly averaged) video image are segmented and identified. Based on a star catalog it is then determined how many stars up to a given magnitude are located inside the field of view. A comparison with the measured star count yields the limiting magnitude. This way, individual stars with exotic spectral classes, double or variable stars have almost no impact anymore.

The operation area of both cameras differs significantly (the noise level of the Watec camera was about 24 brightness levels compared to only 6 for the Mintron),

Figure 4 – Left: fireball on 2014 March 2, $00^h21^m16^s$ UT, recorded by Antal Igaz with Hudeb. Right: fireball on 2014 March 8, $01^h20^m54^s$ UT, recorded by Rui Goncalves with Templar5.

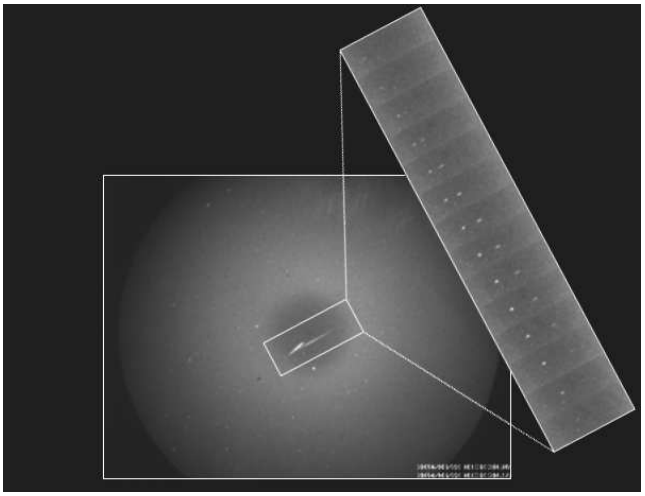

Figure 5 – A nice double-meteor recorded by Detlef Koschny on 2014 March 21, $03^h32^m20^s$ UT with Lic4. The zoomed-in image shows the temporal development.

but the software will automatically adapt to that. For the Watec camera about 100 stars could be identified, which yielded a limiting magnitude of +5.5 magnitude. At the same time, only about 70 stars were found in the Mintron recording, which yielded +5.1 magnitude. So if you push the Watec 910HX-RC to the limits, it is indeed almost half a magnitude more sensitive than the Mintron 12V6-EX.

By chance, the Watec also recorded a faint meteor in the short interval, and that made us a little concerned since it was not well-defined but appeared a little fuzzy and unfocused. Is the Watec camera in fact cheating by integrating over more than two frames in a sliding fashion? To be sure we conducted a few experiments with an "artificial meteor" (laser pointer) which did not increase our suspicion. It seems only by chance that we recorded one of those rare meteors which slowly disintegrate in full view of the observer.

What other differences are there between the Mintron and Watec camera?

- The housing of the Mintron is compact, but the Watec is really tiny. You can hardly build the camera any smaller.
- Both cameras offer frame integration, which is only of limited help for meteor observers but interesting for other astronomical purposes.
- Both cameras are configured via OSD (on-screen display) with five push-buttons. The buttons of the Mintron are directly integrated in the back of the housing. The Watec leaves you the choice between a model where the buttons are integrated into the housing as well, and the RC edition which comes with a small remote control connected via cable. That is very comfortable for the initial configuration of the camera, but a meteor observer will do the settings only once and never touch them again, which minimizes this advantage.
- Whereas the Mintron has only two settings for gamma correction (0.45 and 1.0), the gamma of the Watec can be set in steps of 0.05 and values smaller than than 0.45 may be selected. Additionally, the contrast may be adjusted linearly by setting the minimum and maximum brightness value. Whether that can be used to further push the sensitivity could not be tested on short notice.
- Both cameras showed a few hot pixels, which you are not happy about when buying a new camera. These pixels were more obvious in case of the Mintron because of the lower noise level.
- If you switch off the AGC (automatic gain control), you can adjust the gain of the Mintron manually. The Watec offers three AGC levels (low, medium and high), and you can set the gain in dB when you switch off AGC.

There are further differences between both cameras, but they are not really relevant to amateur astronomers.

Overall we can conclude that the Mintron costs significantly less than the Watec and yields more "aesthetic" pictures, but that comes at the cost of almost half a magnitude. It should also be noted that the latest edition of the Watec, with serial numbers beyond 1000, is said to be even more sensitive. Both cameras are well suited for meteor observation and in the end the observer has to decide which camera he prefers.

Handling Editor: Javor Kac

Table 1 – Observers contributing to 2014 March data of the IMO Video Meteor Network. Eff.CA designates the effective collection area.

Code	Name	Place	Camera	FOV [°²]	Stellar LM [mag]	Eff.CA [km²]	Nights	Time [h]	Meteors
ARLRA	Arlt	Ludwigsfelde/DE	Ludwig2 (0.8/8)	1534	5.8	2467	26	185.7	318
BERER	Berkó	Ludányhalászi/HU	Hulud1 (0.8/3.8)	5542	4.8	3847	12	100.5	285
			Hulud3 (0.95/4)	4357	3.8	876	4	31.4	23
BOMMA	Bombardini	Faenza/IT	Mario (1.2/4.0)	5794	3.3	739	23	119.0	303
BREMA	Breukers	Hengelo/NL	Mbb3 (0.75/6)	2399	4.2	699	24	200.1	173
			Mbb4 (0.8/8)	1470	5.1	1208	22	158.5	131
BRIBE	Klemt	Herne/DE	Hermine (0.8/6)	2374	4.2	678	28	181.7	254
		Bergisch Gladbach/DE	Klemoi (0.8/6)	2286	4.6	1080	25	196.2	242
CASFL	Castellani	Monte Baldo/IT	Bmh1 (0.8/6)	2350	5.0	1611	24	217.7	419
			Bmh2 (1.5/4.5)*	4243	3.0	371	25	210.3	294
CRIST	Crivello	Valbrevenna/IT	Bilbo (0.8/3.8)	5458	4.2	1772	27	147.9	316
			C3P8 (0.8/3.8)	5455	4.2	1586	24	164.7	171
			Stg38 (0.8/3.8)	5614	4.4	2007	24	182.5	372
DONJE	Donani	Faenza/IT	Jenni (1.2/4)	5886	3.9	1222	25	180.3	418
ELTMA	Eltri	Venezia/IT	Met38 (0.8/3.8)	5631	4.3	2151	22	118.4	187
FORKE	Förster	Carlsfeld/DE	Akm3 (0.75/6)	2375	5.1	2154	3	22.4	35
GANKA	Gansel	Dingden/DE	Daro01 (1.4/3.6)	7141	3.1	652	20	129.4	174
GONRU	Goncalves	Tomar/PT	Templar1 (0.8/6)	2179	5.3	1842	23	192.8	346
			Templar2 (0.8/6)	2080	5.0	1508	23	198.1	321
			Templar3 (0.8/8)	1438	4.3	571	26	196.4	168
			Templar4 (0.8/3.8)	4475	3.0	442	21	177.4	237
			Templar5 (0.75/6)	2312	5.0	2259	26	185.9	243
GOVMI	Govedič	Središče ob Dravi/SI	Orion2 (0.8/8)	1447	5.5	1841	25	182.1	267
			Orion3 (0.95/5)	2665	4.9	2069	12	74.0	90
			Orion4 (0.95/5)	2662	4.3	1043	23	53.8	143
HERCA	Hergenrother	Tucson/US	Salsa3 (1.2/4)*	2198	4.6	894	29	287.1	346
IGAAN	Igaz	Baja/HU	Hubaj (0.8/3.8)	5552	2.8	403	13	90.0	88
		Debrecen/HU	Hudeb (0.8/3.8)	5522	3.2	620	26	207.9	206
		Hódmezővásárhely/HU	Huhod (0.8/3.8)	5502	3.4	764	26	168.1	163
		Budapest/HU	Hupol (1.2/4)	3790	3.3	475	21	58.7	55
JONKA	Jonas	Budapest/HU	Husor (0.95/4)	2286	3.9	445	25	149.1	164
KACJA	Kac	Ljubljana/SI	Orion1 (0.8/8)	1402	3.8	331	15	69.0	47
		Kamnik/SI	Cvetka (0.8/3.8)*	4914	4.3	1842	21	147.6	420
			Rezika (0.8/6)	2270	4.4	840	18	131.3	419
			Stefka (0.8/3.8)	5471	2.8	379	20	156.0	279
		Kostanjevec/SI	Metka (0.8/12)*	715	6.4	640	8	70.8	157
KISSZ	Kiss	Sülysáp/HU	Husul (0.95/5)*	4295	3.0	355	22	134.1	62
KOSDE	Koschny	Izana Obs./ES	Icc7 (0.85/25)*	714	5.9	1464	20	143.7	820
		La Palma/ES	Icc9 (0.85/25)*	683	6.7	2951	25	165.5	954
		Noordwijkerhout/NL	Lic4 (1.4/50)*	2027	6.0	4509	16	118.1	195
LOJTO	Łojek	Grabniak/PL	Pav57 (1.0/5)	1631	3.5	269	18	132.2	100

Table 1 – Observers contributing to 2014 March data of the IMO Video Meteor Network – continued from previous page.

Code	Name	Place	Camera	FOV [°2]	Stellar LM [mag]	Eff.CA [km^2]	Nights	Time [h]	Meteors
MACMA	Maciejewski	Chełm/PL	Pav35 (0.8/3.8)	5495	4.0	1584	19	135.6	268
			Pav36 (0.8/3.8)*	5668	4.0	1573	20	158.1	300
			Pav43 (0.75/4.5)*	3132	3.1	319	19	115.3	74
			Pav60 (0.75/4.5)	2250	3.1	281	20	125.0	202
MASMI	Maslov	Novosibirsk/RU	Nowatec (0.8/3.8)	5574	3.6	773	16	90.4	221
MOLSI	Molau	Seysdorf/DE	Avis2 (1.4/50)*	1230	6.9	6152	20	163.3	777
			Mincam1 (0.8/8)	1477	4.9	1084	27	222.3	344
		Ketzür/DE	Remo1 (0.8/8)	1467	6.5	5491	27	186.8	586
			Remo2 (0.8/8)	1478	6.4	4778	25	198.6	471
			Remo3 (0.8/8)	1420	5.6	1967	12	85.2	46
			Remo4 (0.8/8)	1478	6.5	5358	27	200.0	515
MORJO	Morvai	Fülöpszállás/HU	Huful (1.4/5)	2522	3.5	532	26	221.4	157
MOSFA	Moschner	Rovereto/IT	Rover (1.4/4.5)	3896	4.2	1292	26	164.7	257
OCHPA	Ochner	Albiano/IT	Albiano (1.2/4.5)	2944	3.5	358	19	93.8	141
OTTMI	Otte	Pearl City/US	Orie1 (1.4/5.7)	3837	3.8	460	19	113.3	187
PERZS	Perkó	Becsehely/HU	Hubec (0.8/3.8)*	5498	2.9	460	26	183.8	278
PUCRC	Pucer	Nova vas nad Dragonjo/SI	Mobcam1 (0.75/6)	2398	5.3	2976	21	152.0	201
ROTEC	Rothenberg	Berlin/DE	Armefa (0.8/6)	2366	4.5	911	17	139.6	140
SARAN	Saraiva	Carnaxide/PT	Ro1 (0.75/6)	2362	3.7	381	24	181.3	192
			Ro2 (0.75/6)	2381	3.8	459	24	184.3	198
			Ro3 (0.8/12)	710	5.2	619	23	184.4	249
			Sofia (0.8/12)	738	5.3	907	24	194.4	154
SCALE	Scarpa	Alberoni/IT	Leo (1.2/4.5)*	4152	4.5	2052	4	25.3	24
SCHHA	Schremmer	Niederkrüchten/DE	Doraemon (0.8/3.8)	4900	3.0	409	27	186.5	328
SLAST	Slavec	Ljubljana/SI	Kayak1 (1.8/28)	563	6.2	1294	13	75.0	44
STOEN	Stomeo	Scorze/IT	Min38 (0.8/3.8)	5566	4.8	3270	25	132.1	394
			Noa38 (0.8/3.8)	5609	4.2	1911	27	159.7	353
			Sco38 (0.8/3.8)	5598	4.8	3306	28	176.4	486
STRJO	Strunk	Herford/DE	Mincam2 (0.8/6)	2354	5.4	2751	25	196.6	344
			Mincam3 (0.8/6)	2338	5.5	3590	23	192.2	270
			Mincam4 (1.0/2.6)	9791	2.7	552	20	137.5	168
			Mincam5 (0.8/6)	2349	5.0	1896	24	185.7	266
			Mincam6 (0.8/6)	2395	5.1	2178	27	190.6	256
TEPIS	Tepliczky	Agostyán/HU	Huago (0.75/4.5)	2427	4.4	1036	26	205.2	194
		Budapest/HU	Humob (0.8/6)	2388	4.8	1607	24	169.6	290
TRIMI	Triglav	Velenje/SI	Sraka (0.8/6)*	2222	4.0	546	17	52.8	148
YRJIL	Yrjölä	Kuusankoski/FI	Finexcam (0.8/6)	2337	5.5	3574	23	140.8	196
ZELZO	Zelko	Budapest/HU	Huvcse03 (1.0/4.5)	2224	4.4	933	13	31.6	65
			Huvcse04 (1.0/4.5)	1484	4.4	573	10	29.0	58
* active field of view smaller than video frame						Overall	31	11 816.6	20 247

Determination of the maximum of the Geminid meteor shower from visual observation

Jozef Drga[1] *and Marián Janek*[2]

In this contribution, the determination of the maximum phase of the Geminid meteor shower from visual observations of the Geminids conducted from 2008 to 2012 is presented. The information about the ZHR (Zenithal Hourly Rate) was downloaded from the IMO website and the description of the ZHR profile is based on the Gaussian distribution function. When the data are fitted with Gaussian and 2nd order polynomial function, the maximum is positioned at $\lambda_\odot = 261\,^\circ\!.957 \pm 0\,^\circ\!.007$; when the data are fitted by two Gaussian functions, the maximum lies at $\lambda_\odot = 261\,^\circ\!.98 \pm 0\,^\circ\!.01$.

Received 2013 January 22

1 Introduction

The Geminids is the most active December meteor shower. It is characterized by over 100 meteors per hour. The radiant maximum position is at $\alpha = 112°$, $\delta = +33°$ and the maximum occurs at $\lambda_\odot = 262\,^\circ\!.2$ (McBeath, 2011). The geocentric velocity of these meteors is $v_g = 35$ km s^{-1} and the population index is $r = 2.6$. The parent body (Whipple, 1983) of this meteor shower is asteroid (3200) Phaethon. Whipple found the relation between 13 photographic Geminid meteors and (3200) Phaethon orbital elements. The possible ejection of dust particles from this body was detected in June 2009 (Jewitt & Li, 2010; Ryabova, 2012). The peak related to this activity is expected after 2014. In 2014, the peak is predicted to occur at $\lambda_\odot = 262\,^\circ\!.5$ and from a theoretical radiant of $\alpha \approx 114\,^\circ\!.65 \pm 2\,^\circ\!.5$, $\delta \approx +32\,^\circ\!.7 \pm 0\,^\circ\!.1$ (Ryabova, 2012). Additional activity was observed again in 2012 as reported in (Li & Jewitt, 2013; Jewitt et al., 2013). Jewitt et al. (2013) do not claim that this activity can explain the current mass of the Geminid stream and it may not be associated with the event(s) that caused the bulk of the Geminid stream (full-blown cometary activity, cascading splitting/disintegration events).

2 Results

The Geminids activity profile was downloaded from the International Meteor Organisation website `www.imo.net` and it is based on the data from 2008 to 2012. The high number of observations allows us to determine the position of the maximum of activity profile peak with relatively high accuracy, which reflects the fact that the maximum occurs at the same solar longitude. The maximum is obtained by fitting the data with the functions:

$$f(x) = A\,(x - B)^2 + C + D\,e^{-\frac{1}{2}\left(\frac{x-\mu}{\sigma}\right)^2} \qquad (1)$$

$$f(x) = A_1\,e^{-\frac{1}{2}\left(\frac{x-\mu_1}{\sigma_1}\right)^2} + A_2\,e^{-\frac{1}{2}\left(\frac{x-\mu_2}{\sigma_2}\right)^2} \qquad (2)$$

where μ and σ are the mean and the standard deviation of the Gaussian, respectively. The fitting procedure is performed on 44 296 Geminid records obtained in 4043 intervals.

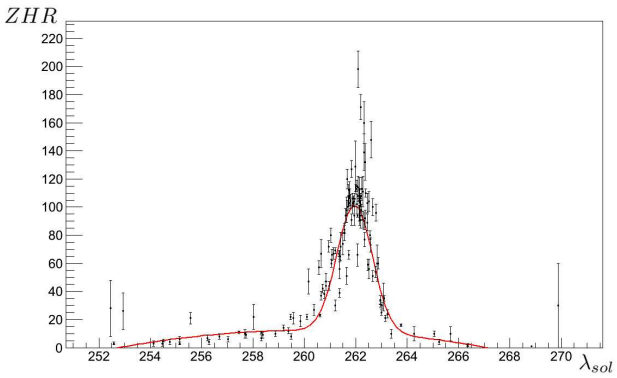

Figure 1 – Dependence of ZHR on solar longitude $\lambda_\odot$. Red curve denotes fitting function (1).

The function (1) shows the maximum at $\lambda_\odot = 261\,^\circ\!.957 \pm 0\,^\circ\!.007$. The Geminids' active phase was calculated from $\lambda_\odot = 252\,^\circ\!.78$ to $\lambda_\odot = 267\,^\circ\!.13$ (from December 3 to 18/19). The reason for choosing this fitting function is that we can obtain the meteor shower activity from it.

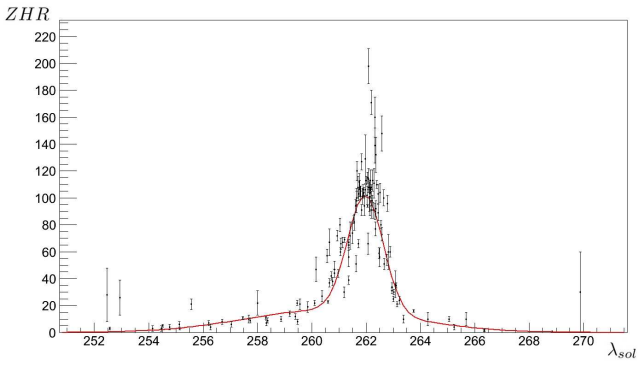

Figure 2 – Dependence of ZHR on solar longitude $\lambda_\odot$. Red curve denotes fitting function (2).

The second approach is based on fitting the data by two Gaussians (2), because the choice of fitting function (1) is not usual. This function based on two Gaussian distributions shows a maximum at $\lambda_\odot = 261\,^\circ\!.98 \pm 0\,^\circ\!.01$. One can see that the solar longitudes obtained by the two methods are very similar.

[1]Alexander Dubček University of Trenčín, Študentská 2, Trenčín, Slovak Republic Email: `dodo.tn@seznam.cz`

[2]Department of Physics, Faculty of Electrical Engineering, University od Žilina, Univerzitná 1, Žilina, Slovak Republic

IMO bibcode WGN-423-drga-geminids
NASA-ADS bibcode 2014JIMO...42..125D

Table 1 – Fitting parameters of Gaussian and 2nd order polynomial function (1).

Parameter	Value	St. deviation
σ	0.688	0.007
μ	261.957	0.007
A	−0.24	0.02
B	260.0	0.1
C	12.2	0.5
D	90.4	0.7

Table 2 – Fitting parameters of two Gaussian functions (2).

Parameter	Value	St. deviation
σ_1	0.66	0.01
μ_1	261.98	0.01
A_1	87	1
σ_2	3.1	0.2
μ_2	260.6	0.2
A_2	16.7	1.0

3 Conclusions

By a fitting procedure, the maximum phase of the Geminid meteor shower was determined. For the evaluation of this maximum, CERN's program Root (Brun & Rademakers, 1997) with the algorithm of MIGRAD type was used. It was found that when the data are fitted with Gaussian and 2nd order polynomial function, the maximum is positioned at $\lambda_\odot = 261\,^\circ\!.957 \pm 0\,^\circ\!.007$, and when the data are fitted by two Gaussian functions, the maximum lies at $\lambda_\odot = 261\,^\circ\!.98 \pm 0\,^\circ\!.01$. These values are in good agreement with value of $262\,^\circ\!.2$ published by McBeath (2011).

References

Brun R. and Rademakers F. (1997). "ROOT – an object oriented data analysis framework". *Nuclear Instruments and Methods in Physics Research A*, **389**, 81–86. (`http://root.cern.ch/`).

Jewitt D. and Li J. (2010). "Activity in Geminid parent (3200) Phaethon". *Astronomical Journal*, **140**, 1519–1527.

Jewitt D., Li J., and Agarwal J. (2013). "The dust tail of asteroid (3200) Phaethon". *Astrophysical Journal Letters*, **771**, L36.

Li J. and Jewitt D. (2013). "Recurrent perihelion activity in (3200) Phaethon". *Astronomical Journal*, **145**, 154.

McBeath A. (2011). "IMO 2012 Meteor Shower Calendar". IMO_INFO(2-11).

Ryabova G. O. (2012). "On the possible ejection of meteoroids from asteroid (3200) Phaethon in 2009". *MNRAS*, **421**, 2254–2259.

Whipple F. L. (1983). "1983 TB and the Geminid meteors". *IAU Circulars*, **3881**.

Handling Editor: Željko Andreić

The International Meteor Organization

web site http://www.imo.net

Council

President: Cis Verbeeck,
Bogaertsheide 5, 2560 Kessel, Belgium.
e-mail: cis.verbeeck@scarlet.be

Vice-President: Jürgen Rendtel,
Eschenweg 16, D-14476 Marquardt, Germany.
tel. +49 33208 50753
e-mail: jrendtel@aip.de

Secretary-General: Robert Lunsford,
1828 Cobblecreek Street, Chula Vista,
CA 91913-3917, USA. tel. +1 619 585 9642
e-mail: lunro.imo.usa@cox.net

Treasurer: Marc Gyssens, Heerbaan 74,
B-2530 Boechout, Belgium.
e-mail: marc.gyssens@uhasselt.be
BIC: GEBABEBB
IBAN: BE30 0014 7327 5911
Always state BIC and IBAN codes together!
Check international transfer charges with your bank; you are responsible for paying these.

Other Council members:

David Asher, Armagh Observatory, College Hill, Armagh, Northern Ireland BT61 9DG, UK.
e-mail: dja@arm.ac.uk

Geert Barentsen, University of Hertfordshire, Hatfield AL10 9AB, UK. e-mail: geert@barentsen.be

Javor Kac (see details under WGN)

Detlef Koschny, Zeestraat 46,
NL-2211 XH Noordwijkerhout, Netherlands.
e-mail: detlef.koschny@esa.int

Sirko Molau, Abenstalstraße 13b, D-84072 Seysdorf, Germany. e-mail: sirko@molau.de

Jean-Louis Rault, Société Astronomique de France, 16, rue de la Vallée, 91360 Epinay sur Orge, France. e-mail: f6agr@orange.fr

Paul Roggemans (see details under IMC Liaison Officer)

Commission Directors

Visual Commission: Rainer Arlt (rarlt@aip.de)
Generic e-mail address: visual@imo.net
Electronic visual report form:
http://www.imo.net/visual/report/electronic

Video Commission: Sirko Molau (sirko@molau.de)
Generic e-mail address: video@imo.net

Photographic Commission: Bill Ward (William.Ward@glasgow.ac.uk)
Generic e-mail address: photo@imo.net

Radio Commission: Jean-Louis Rault (f6agr@orange.fr)
Generic e-mail address: radio@imo.net

Fireballs: Online fireball reports: coming soon

IMC Liaison Officer

Paul Roggemans, Pijnboomstraat 25, 2800 Mechelen, Belgium, e-mail: paul.roggemans@gmail.com

WGN

Editor-in-chief: Javor Kac
Na Ajdov hrib 24, SI-2310 Slovenska Bistrica, Slovenia. e-mail: wgn@imo.net;
include METEOR in the e-mail subject line

Editorial board: Ž. Andreić, R. Arlt, D.J. Asher, J. Correira, M. Gyssens, H.V. Hendrix, C. Hergenrother, J. Rendtel, J.-L. Rault, P. Roggemans, C. Trayner, C. Verbeeck.

IMO Sales

Available from the Treasurer or the Electronic Shop on the IMO Website	€	$
IMO membership, including subscription to WGN Vol. 42 (2014)		
Surface mail	26	39
Air Mail (outside Europe only)	49	69
Electronic subscription only	21	29
Back issues of WGN on paper (price per complete volume)		
Vols. 26 (1998) – 35 (2007) except 30 (2002), 38 (2010) – 41 (2013)	15	23
Vols. 37 (2009) – 41 (2013) – electronic version only	9	13
Proceedings of the International Meteor Conference on paper		
1990, 1991, 1993, 1995, 1996, 1999, 2000, 2002, 2003, per year	9	13
2007, 2010, 2011, per year	15	23
2012	25	37
Proceedings of the Meteor Orbit Determination Workshop 2006	15	23
Radio Meteor School Proceedings 2005	15	23
Handbook for Meteor Observers	20	29
Electronic media		
Meteor Beliefs Project CD-ROM	6	9
DVD: WGN Vols. 6–30 & IMC 1991, 1993–96, 2001–04	45	69

Activity and Observability of Meteor Showers throughout the Year

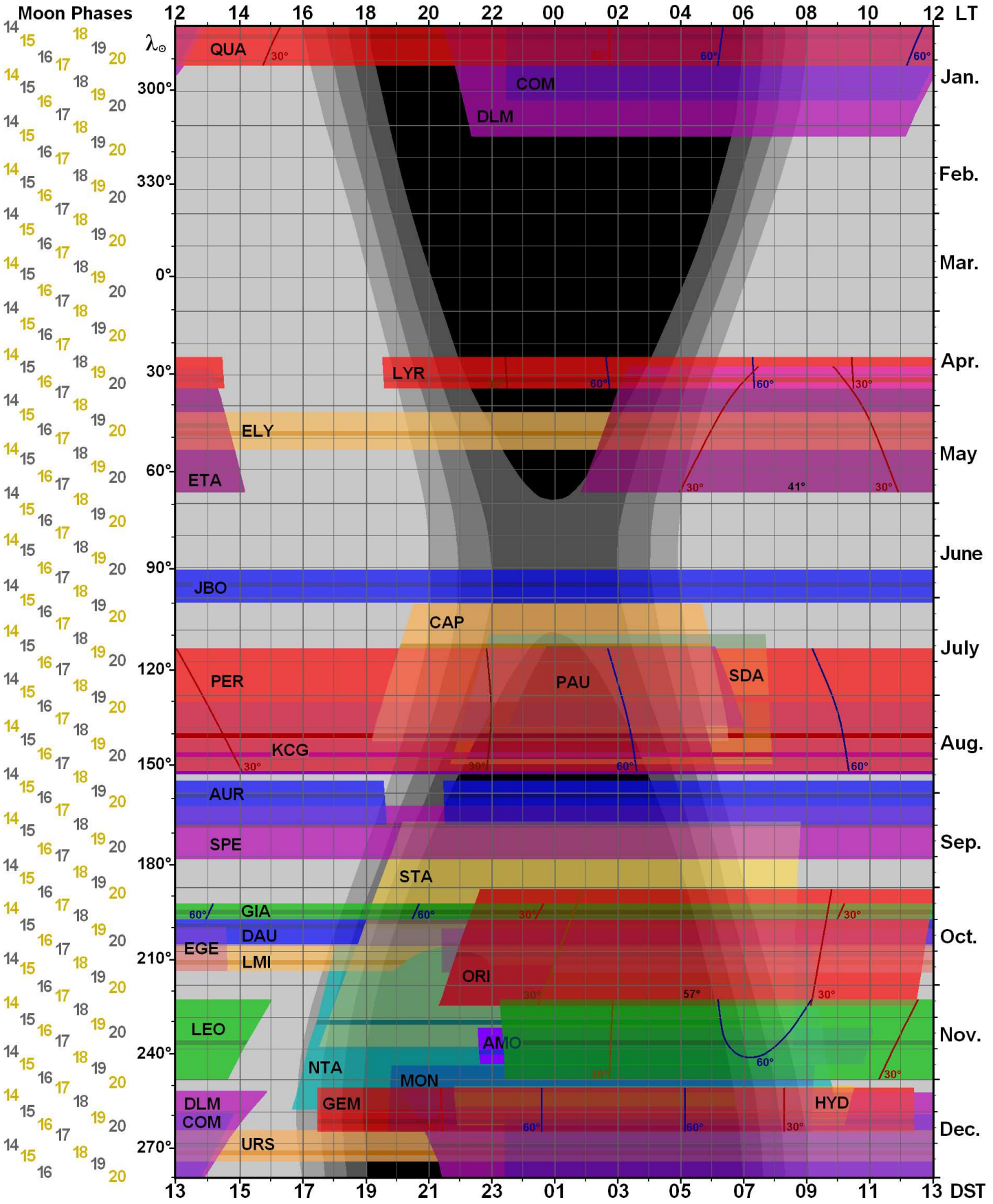

The diagram presents the activity periods of meteor showers as well as the rise and setting times of meteor shower's radiants. Plotted are sunrises, sunsets and the period of twilight, too. It was constructed according to data from IMO Meteor Shower Working List. More active showers are displayed in red or green colour, respectively. For these showers times are plotted when radiant reaches altitudes of 30° and 60°The maxima of showers are drawn as belt with darker shade of corresponding colour. The diagram is calculated for geographic latitude of 50° N. Time scale is given as local time at relevant zonal meridian and supplemented by local daylight saving time, too. The diagram contains round values of solar longitude J2000 and Moon phases from 2014 to 2020. Full Moons are symbolized by a yellow number and New Moons by a grey one. Courtesy of Peter Zimnikoval.